


CFD Simulation of flow through pipe fittings

Internship Report
CFD-FOSSEE Team
Indian Institute of Technology Bombay

Prepared by
Mukund S
BMS College of Engineering, Banglore

Under the supervision of

Prof. Manaswita Bose

INDIAN INSTITUTE OF TECHNOLOGY BOMBAY


ACKNOWLEDGEMENT

The following report was created as a part of FOSSEE semester long internship and I would like to thank FOSSEE, Indian Institute of Technology, Bombay for giving me this opportunity.

I would like to thank my project guide Prof. Manaswita Bose, Mentors Mr. Divyesh Variya and Mr. Ashley Melvin for the support in carrying out simulations through out the internship. I would also like to thank project manager Ms. Swetha Manian for giving me this opportunity.

I would like to extend my gratitude to Head, Department of Energy Science and Engineering, Indian Institute of Technology Bombay for giving the permission to use experimental data for validation and Swapnil Raut for helping with details and support.

Mukund S
BMS College of Engineering, Banglore
Date: August 23, 2021

Contents

List of Figures

List of Tables

Part I

Case Study 1: Coefficient of Discharge of an Orifice Meter

Chapter 1

Introduction

1.1 Aim

The aim of this case study was to determine the Coefficient of discharge of an orifice meter through CFD method. OpenFOAM version 1912 was used for carrying out the simulation. Further, the velocity and pressure contours of the flow were studied and the position of the vena contracta was characterized. The study was performed for a 2-D incompressible flow with water as the working fluid, simpleFoam steady state solver was used and κ-ϵ RANS model was adopted to simulate the turbulent flow. The results were viewed in ParaView 5.7.0

1.2 Theory

An orifice meter is essentially a cylindrical tube that contains a plate with a thin hole in the middle of it. The thin hole essentially forces the fluid to flow faster through the hole in order to maintain flow rate. The point of maximum convergence (vena contracta) usually occurs slightly downstream from the actual physical orifice. This is the reason why orifice meters are less accurate than venturi meters, as we cannot use the exact location and diameter of the point of maximum convergence in calculations. Beyond the vena contracta point, the fluid expands again and velocity decreases as pressure increases. Figure 1.1 shows an orifice meter with the variable position of vena contracta with respect to the orifice plate. By employing the continuity equation and Bernoullis principle, the volumetric flow

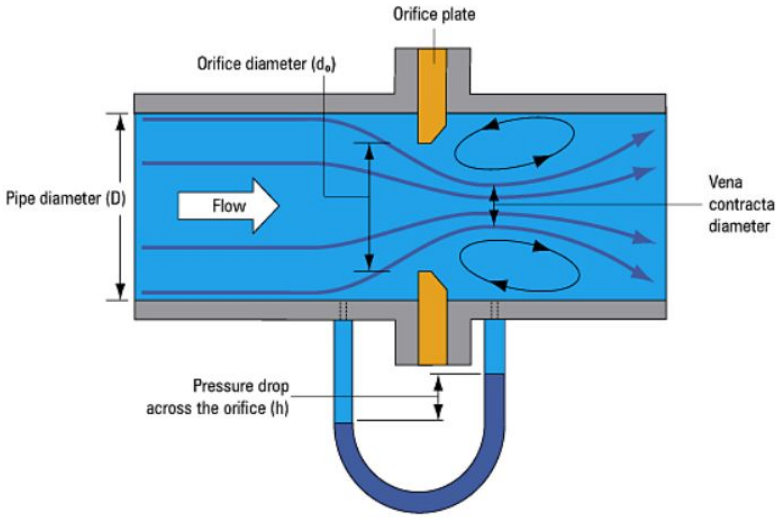

Figure 1.1: Orifice meter [1]

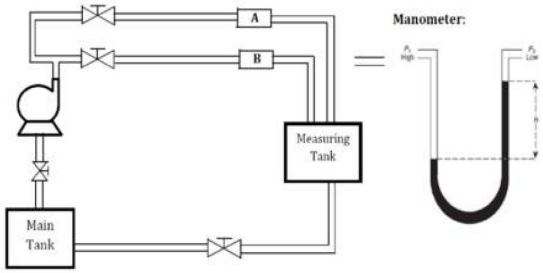

Figure 1.2: Schematic Diagram for Orifice meter B: Orifice meter [2]

rate through the orifice meter can be calculated giving the below equation,

$$Q = V_2 S_2 = \frac{C_O S_2 \sqrt{2g\delta H}}{\sqrt{1-\beta^4}} \tag{1.1}$$

where C_O is the orifice discharge coefficient, S_2 is the area of cross-section of the orifice, V_2 is the flow velocity through the orifice, β is the ratio of the orifice diameter to that of the pipe, δH is the manometric height difference Œ (specific gravity of manometric fluid specific gravity of water), and g is the acceleration due to gravity. Figure 1.2 depicts the schematic layout of the test setup consisting of the orifice meter [4] [5].

1.3 Problem Statement

The primary objective of the case study is to simulate turbulent flow inside an orifice meter and later calculate the coefficient of discharge using the CFD result and compare it with the experimental results. The dimensions of the orifice geometry are considered from the lab manual. The simulations were conducted for 15 different cases with reynolds number varying from the range of 6000 to 20000. To study this turbulent flow, simpleFoam solver is used.

1.4 Schematic Diagram

The dimensions of the geometry is given below
Length of the orifice meter = 13mm
Entrance diameter, D1 = 16mm
Diameter of the orifice, D2= 8mm
Cross-sectional area of the orifice, $S_2 = \frac{\pi(D_2)^2}{4} = 5.026 \times 10^{-5}$
$\beta = \frac{D_2}{D_1} = 0.5$
The geometry of the orifice meter is shown in the Figure 1.3.

Figure 1.3: Axisymmetric Geometry of orifice meter

Chapter 2

OpenFOAM base case

2.1 pitzDaily

The base case considered for the simulation of the orifice meter is the pitzDaily case. This case can be found under the incomressible section, simpleFoam subsection. The directory for this is
\OpenFOAM-v1912\tutorials\incompressible\simpleFoam\pitzDaily.
Based on the experimental work of Pitz and Daily (1981). It features a backward facing step. Such a "classic" case is instructive for comparing different turbulence models with respect to the size and shape of the recirculation zone[internet reference]. pitzDaily introduces the dollowing concepts for the first time:

- Mesh creation using blockMesh and also mesh grading capability
- Turbulent steady flow.

2.1.1 Folder Structure

Any case file in OpenFOAM has three folders, called the 0, constant and the system. The constant contains coefficient values that will be used in equations and also things which will remain constant like the mesh, material properties, environmental constants which the solver uses, the 0 folder contains the initial and boundary conditions, and the system folder contains the configuration files for the mesh and also how the solver will be executed, schemes and methods to use and controls for the simulation.

Table 2.1: Folder contents

Directories	Constant	0	System
Sub-directories	transportProperties turbulenceProperties polyMesh	U p nut epsilon k	blockMeshDict fvSchemes fvSolution

2.2 Solver

OpenFOAM or Open-source Field Operation And Manipulation is an open-source C++ tool used for solving continuum mechanics problems, with a focus on Finite Volume Method (FVM). The software package includes solver codes for different kinds of transport phenomena, varying from simple laplacian solver called laplacianFoam to complex multiphase flow, compressible flow, heat transfer, incompressible flow, and many more. The flagship solver and most commonly used solver is simpleFoam. simpleFoam is a steady-state solver for incompressible, turbulent flow. It utilizes the SIMPLE (Semi-Implicit Method for Pressure Linked Equations) algorithm. It is an approximation of the velocity field which is obtained by solving the momentum equation. The pressure gradient term is calculated using the pressure distribution from the previous iteration or an initial guess. The pressure equation is formulated and solved to obtain the new pressure distribution. Velocities are corrected and a new set of conservative fluxes is calculated. The solver used for this case study is simpleFoam, it employs SIMPLE algorithm. The case study considered is a steady state, incompressible, three-dimensional flow. The set of Navier Stokes equations governing the flow is given below.
The continuity equation is given as,

$$\nabla.\vec{u} = 0 \tag{2.1}$$

The momentum equation is given as.

$$\frac{\partial \vec{u}}{\partial t} + \nabla.[\vec{u}\vec{u}] = -\frac{1}{\rho}\nabla p + \nu\nabla^2\vec{u} \tag{2.2}$$

Where, $\vec{u}$ is velocity, p-pressure; ν is kinematic viscosity The discretized momentum equation and pressure correction equation are solved implicitly, where the

velocity correction is solved explicitly. This is the reason why it is called "Semi-Implicit Method".

2.2.1 Turbulence Model

The turbulence model considered for the simulation is κ -ϵ RANS model. κ -ϵ model solves two additional equations, for turbulent kinematic energy κ and rate of dissipation of turbulence energy ϵ It performs poorly for complex flows involving severe pressure gradient, separation, strong streamline curvature. Suitable for initial iterations, initial screening of alternative designs, and parametric studies. Can be only used with wall functions. The equations for the κ -ϵ RANS model is below,

$$\frac{\partial(p\kappa)}{\partial t} + \frac{\partial(p\kappa u_i)}{\partial x_i} = \frac{\partial}{\partial x_j}[\frac{\mu_t}{\sigma_\kappa}\frac{\partial \kappa}{\partial x_j}] + 2\mu_t E_{ij}E_{ij} - \rho\epsilon \tag{2.3}$$

$$\frac{\partial(p\epsilon)}{\partial t} + \frac{\partial(p\epsilon u_i)}{\partial x_i} = \frac{\partial}{\partial x_j}[\frac{\mu_t}{\sigma_\kappa}\frac{\partial \kappa}{\partial x_j}] + C_{1\epsilon}\frac{\epsilon}{\kappa}2\mu_t E_{ij}E_{ij} - C_{2\epsilon}\rho\frac{\epsilon^2}{\kappa} \tag{2.4}$$

where u_i represents velocity component in corresponding direction, E_{ij} represents component of rate of deformation, and μ_t represents eddy viscosity. The default value of model coefficients [6]: $C_{1\epsilon}$, $C_{2\epsilon}$, σ_κ, σ_ϵ and $C\mu$ have been used.

Chapter 3

OpenFOAM Case Modifications

Using the pitzDaily case, modifications were made with the geometry, the mesh used, boundary conditions applied to it, and the control parameters which are going to be explained further in the below sections.

3.1 Pre-processing

The model was created using the dimensions from the manual provided. To simplify the calculation an axisymmetric wedge was created. In OpenFOAM to make the axisymmetric wedge the angle should be 5 degrees. The upstream length and downstream length was taken to be 320mm and axis along Z direction.
The mesh and geometry was created using the blockMesh utility. The blockMeshDict file from the base case was modified to create the axisymmetric model of the orifice geometry. convertToMeters, the very first line of blockMeshDict file is changed, by default the units used in OpenFOAM are in meters. Since the geometry is in millimetres a conversion factor from meters to millimetres was used, replacing 0.01 to 0.001.
The co-ordinates of the geometry are entered in the vertices column of the file. It is entered as x, y, and z coordinate values. X represents the radial distance; Y represents the angular axis and Z represents the axial length of the geometry. Therefore the coordinate axis can be obtained by simple trigonometric formula of $tan = \frac{Oppositeside}{adjacentside}$. The geometry is divided into blocks for Meshing purposes. There are totally 5 blocks. It was made using hexahedral blocks with simplegrading 1 in all directions. In the axisymmetric geometry, the front, back panels, and the axis are additional boundaries. Proper patchfields are assigned to them, for

the front and back panels, boundary patch assigned is wedge and for the axis it is given as empty. Using the blockMesh utility, the mesh was generated and with checkMesh, the quality of the mesh was determined.

3.2 Boundary conditions

The initial and boundary conditions are included in the 0 folder as k, epsilon, nut,p, and U. The boundary conditions are summarised in the Table 3.1. In all the files

Table 3.1: Boundary conditions

	inlet	outlet	wall
epsilon	turbulentMixingLengthDissipationRateInlet	zeroGradient	epsilonWallFunction
k	turbulentIntensityKineticEnergyInlet	zeroGradient	kqRWallFunction
nut	calculated	calculated	nutkWallFunction
p	zeroGradient	fixedValue	zeroGradient
U	flowRateInletVelocity	zeroGradient	noSlip

in 0 folder, the axis, front_back_pos and front_back_neg were given the boundary condition of empty, wedge and wedge respectively. The value for κ and ϵ were determined using the below equations

$$\kappa = \frac{3}{2}(uI)^2 \tag{3.1}$$

$$\epsilon = \frac{C_\mu \kappa^{1.5}}{0.07l} \tag{3.2}$$

where u is the free stream velocity, I is the turbulence intensity, C_μ is the model coefficient, l is the characteristic length.

3.3 Physical properties

The working fluid for the simulation is water. The density considered is 1000 kg/ m^3, with a kinematic viscosity of 1×10^{-06} m^2/s. So the value in the transportProperties file was changed to 1×10^{-06} from 1×10^{-05} and the transportModel remained as it is to Newtonian.

3.4 fvSchemes & fvSolution

fvSchems and fvSolutions are found under the constant folder. fvSolution directory contains equation solvers, algorithms and tolerances. No changes were done to this file, the tolerances for the residuals were pre-set to a value of 1e-05 and it was not changed. The numerical schemes for the simulation are entered in the fvSchemes dictionary. No changes were made in this file directory.

3.5 Control parameters

The OpenFOAM solvers begin all runs by setting up a database. The database controls I/O and, since output of data is usually requested at intervals of time during the run, time is an inextricable part of the database. The controlDict dictionary sets input parameters essential for the creation of the database. Here the endTime was changed to 10000, i.e., maximum iterations were 10000. startTime was 0 and writeInterval was set to every 100 iterations with 1 as deltaT as it was a steady state analysis.

3.6 Post-processing

After the simulation has been completed, the results were viewed in ParaView. To do this, first the results obtained were converted into viewable file using the command *touch suitable_file_name.foam*. A file with .foam extension was created. In this file, the results was viewed, the various contours of the solution was visualised, streamlines were plotted and the data were analysed with the in-built plotting options available.

Chapter 4

Results

Steady state simulations were performed using SIMPLE algorithm for κ -ϵ RANS model. The obtained CFD results have been compared with the experimental results for the coefficient of discharge. Post-processing was done using paraview.

4.1 Numerical Results

The post-processing of the simulation was done in ParaView for all the 15 simulations. The pressure and velocity contours of the simulation is shown below.

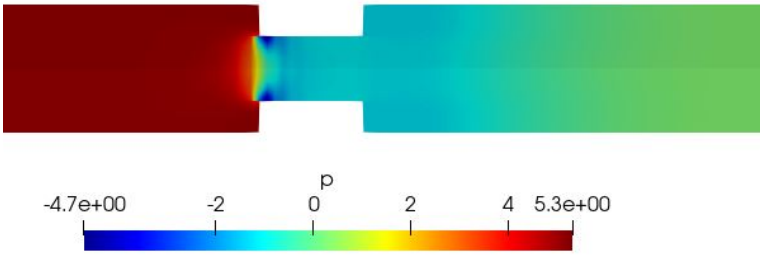

Figure 4.1: Pressure contour

As we can see form the Figure 4.1 and Figure 4.2, as the water flows from a narrowing orifice plate, the flow forms a free flowing jet in the downstream fluid. The velocity is at its maximum. The separation of boundary layer is seen at the downstream side of orifice plate. The turbulent and wake region, together with re-circulation zones can be seen just downstream of orifice meter[7]. Figure 4.3-

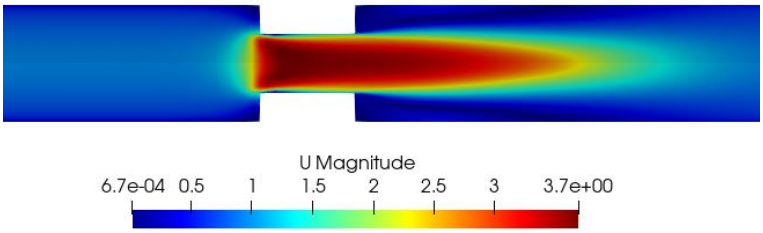

Figure 4.2: Velocity contour

Figure 4.6 show pressure and velocity contours for two different Reynolds number regime. Figure 4.3 and 4.4 are for Reynolds number of 15090, and Figure 4.5 and 4.6 are for Reynolds number of 10650.

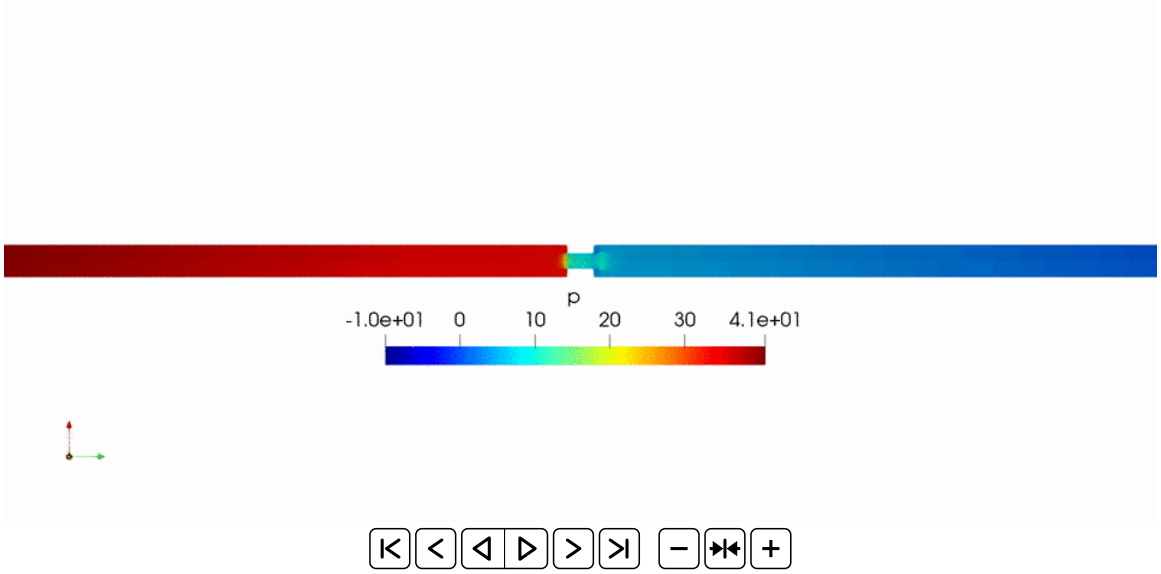

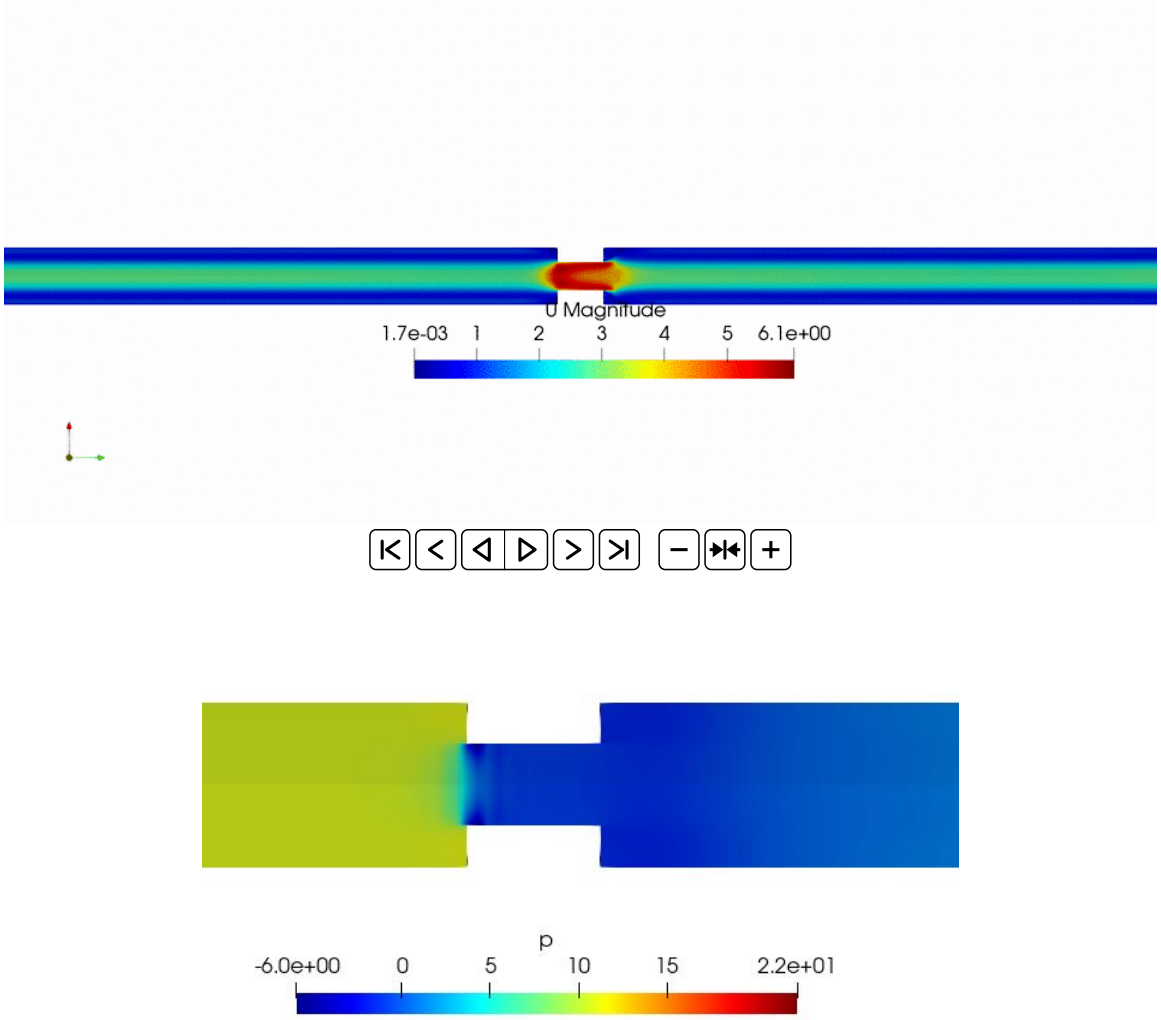

Figure 4.3: Pressure contour for higher Reynolds number

Figure 4.7 shows the developed velocity profile upstream of orifice just before the entrance. Due to the no-slip condition, there is velocity gradient near the walls. This region is often very thin, and it is then called a boundary layer [7]. This graph tells us the velocity is developed and adequate length is given the downstream for the pressure recovery. The evolution of the solution for pressure and velocity is shown above. The pressure was plotted along the axis length as shown in Figure 4.8. The pressure just before the orifice is high and after the orifice there is drop in the pressure. This corresponds to the pressure contour in the Figure 4.1. Figure 4.9 shows the velocity along the axial length of the orifice meter. The velocity remains constant until the mouth of the orifice and then there is a sudden increase as the

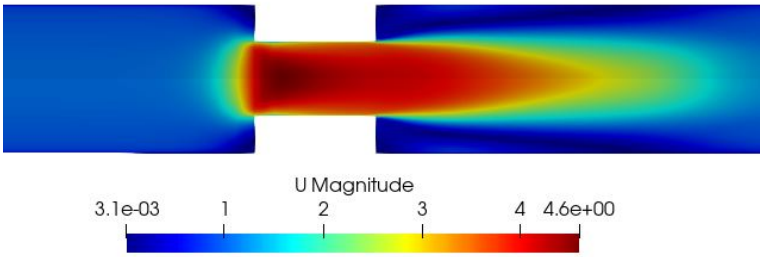

Figure 4.4: Velocity contour for higher Reynolds number

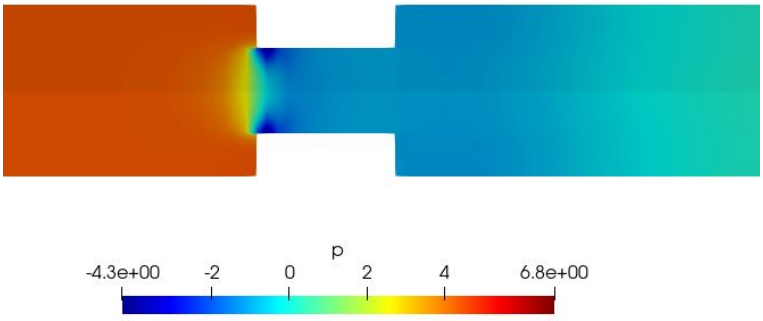

Figure 4.5: Pressure contour for lower Reynolds number

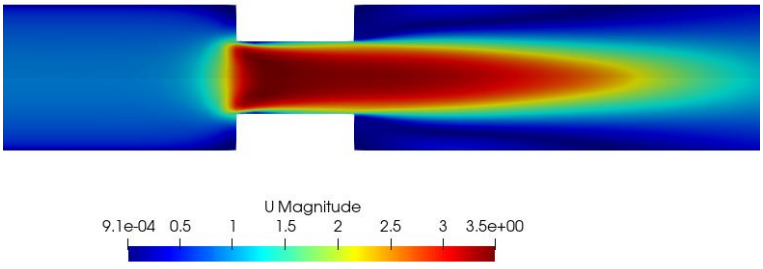

Figure 4.6: Velocity contour for lower Reynolds number

fluid enters the orifice plate. The maximum region of the velocity is called as the vena-contracta and can be seen in velocity contour, Figure 4.2. The streamlines for

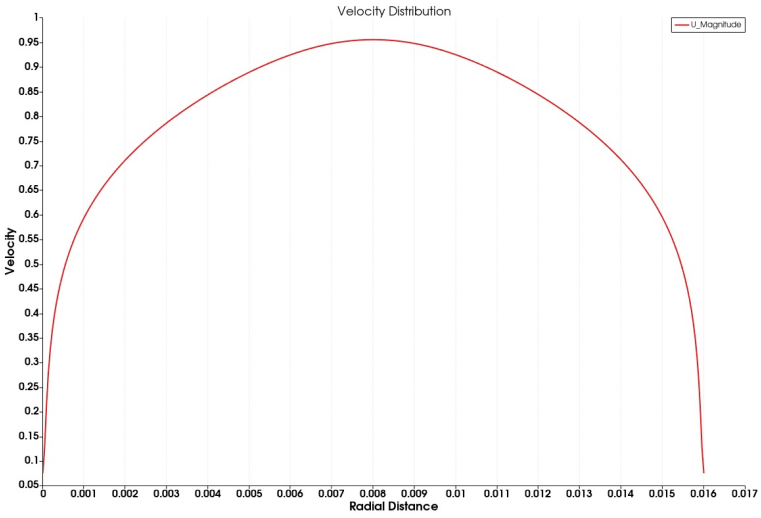

Figure 4.7: Velocity distribution

the flow through the orifice is shown in Figure 4.10. Streamlines for higher and lower Reynolds number cases are shown in Figure 4.11 and 4.12. Vectors were plotted to get a better understanding of the flow as shown in Figure 4.13. Vector plots for higher and lower Reynolds number cases are shown in Figure 4.14 and 4.15 The re-circulation regions are better visualized in the vector plots, and they are circled in red color. Here we can see that the flow converges when it enters the orifice and is accelerated, and at the exit of the orifice the flow expands and diverges, leading to high pressure region. The coefficient of discharge from the CFD results was calculated with pressure predicted by CFD between upstream of orifice and vena-contracta at which the wall pressure is minimum[8]. The same procedure was carried out for all the other simulations by changing the input values in the U, k and epsilon folder and varying changing the number of cells in the mesh.

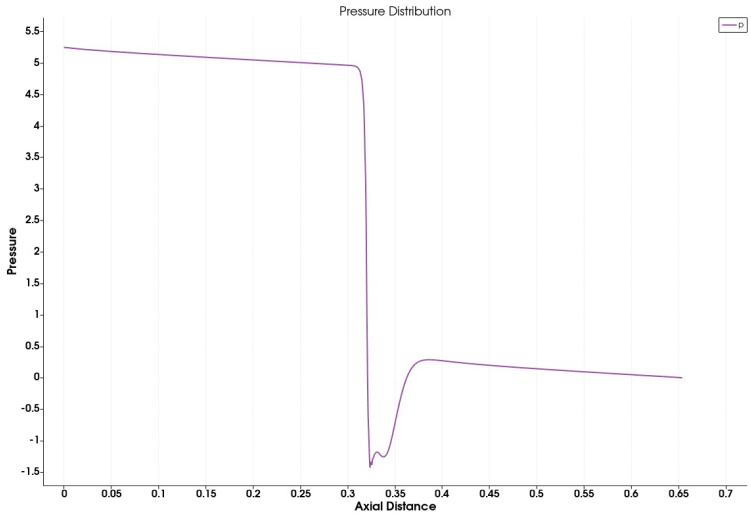

Figure 4.8: Pressure along the axial length

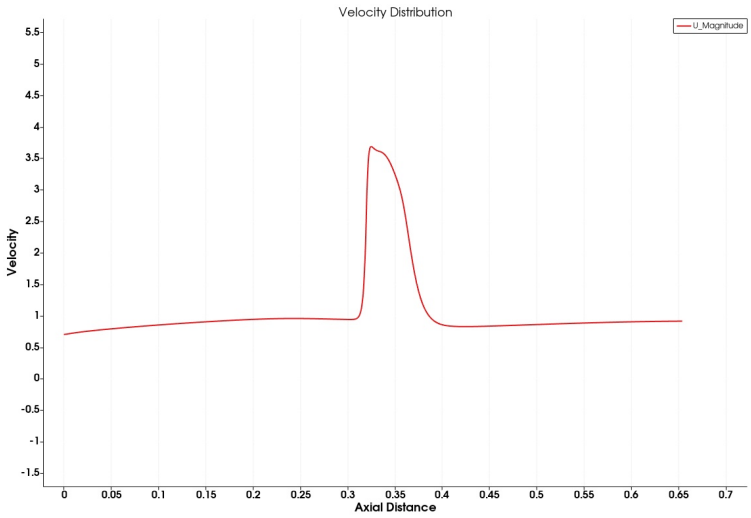

Figure 4.9: Velocity along the axial length

4.2 Experimental Results

The experimental data was provided in the manual [2]. The initial and final height of the collecting tank and the manometer's height difference was given. Using the collecting tanks reading, the flow rate was determined and the pressure head was determined using manometer's height difference. With Equation 6.1, the discharge coefficient for experiment data was determined.

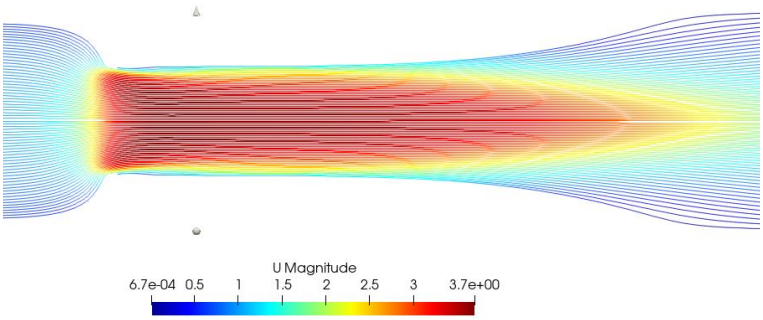

Figure 4.10: Streamlines with velocity scale

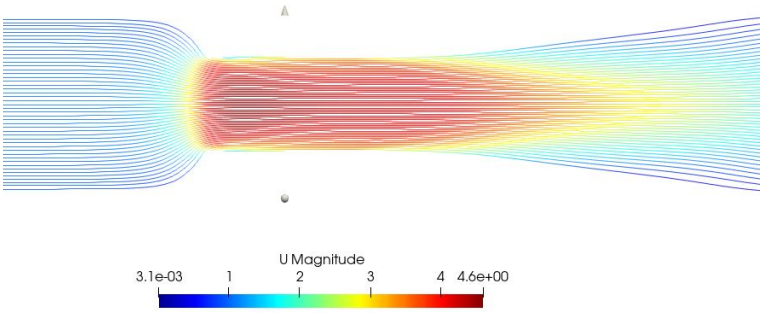

Figure 4.11: Streamlines with velocity scale for higher Reynolds number of 15090

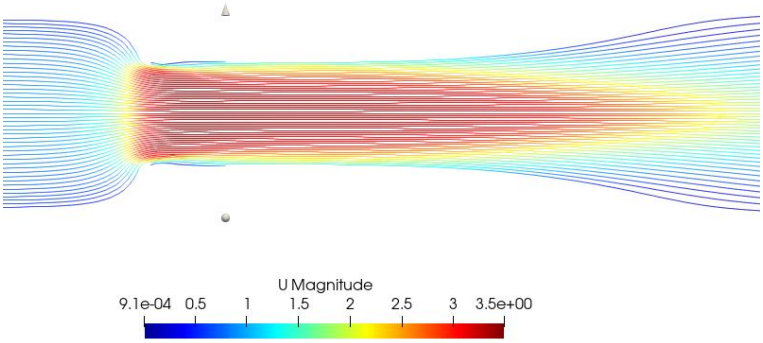

Figure 4.12: Streamlines with velocity scale for lower Reynolds number of 10650

4.3 Result comparison

Both the results obtained, CFD and experimental were compared and is summarised in the Table 4.2 with the input initial conditions for CFD simulations.

Figure 4.13: Vector Plot

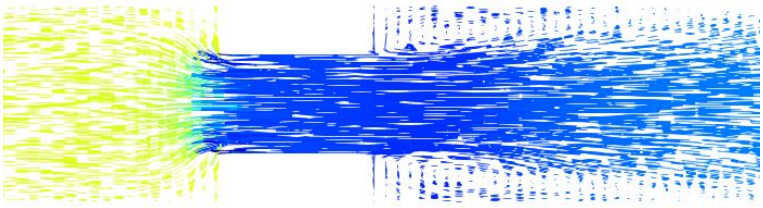

Figure 4.14: Vector Plot for higher Reynolds number of 15090

Figure 4.15: Vector Plot for lower Reynolds number of 10650

From the table we can see that the CFD results obtained is very close to the experimental results. From the table, it can be seen that for Reynolds number greater than 20000, the coefficient of discharge determined was in the range of 0.6-0.66, and for the simulations below this value had the value in the range of 0.7-0.75. To refine the result, two case with low Reynolds number in the range of 6000-8000 was considered and were simulated with low Reynolds number wall boundary

Table 4.1: Low Reynolds number wall boundary conditions

	inlet	outlet	wall
epsilon	turbulentMixingLengthDissipationRateInlet	zeroGradient	epsilonWallFunction
k	turbulentIntensityKineticEnergyInlet	zeroGradient	kLowReWallFunction
nut	calculated	calculated	nutLowReWallFunction
p	zeroGradient	fixedValue	zeroGradient
U	flowRateInletVelocity	zeroGradient	noSlip

conditions which is summarised in Table 4.1. In all the files in 0 folder, the axis, front_back_pos and front_back_neg were given the boundary condition of empty, wedge and wedge respectively. The discharge coefficient obtained did not vary much from the previous simulation.

Table 4.2: Experimental and CFD results

Sl No.	Flow rate(m^3/s)	Velocity (m/s)	Flow rate(m^3/s) for 5^0 wedge	Reynolds number	Turbulent kinetic energy (m^2/s^2)	Turbulent dissipation (m^2/s^3)	Pressure difference	C_D	C_D (exp)
1	0.000141688	0.70491478	1.96789E-06	11278.56	1.8484e-3	6.386e-3	6.6148	0.75	0.6771
2	0.00015124	0.752436107	2.10055E-06	12038.4	2.0724e-3	7.58e-3	7.55	0.749	0.6793
3	0.000171306	0.852269612	2.37925E-06	13636.313	2.51e-3	1.01e-2	10.99039	0.7038	0.7012
4	0.000181862	0.904786907	2.52586E-06	14475.2	2.86e-3	1.2317e-2	10.99742	0.746	0.6981
5	0.00020152	1.00258698	2.79889E-06	16040	3.416e-3	1.6e-2	13.23151	0.7545	0.7378
6	0.000204571	1.017767353	2.84127E-06	16283.2	3.52e-3	1.67e-2	14.10243	0.7417	0.6318
7	0.000189579	0.943181434	2.63305E-06	15089.6	3.07e-3	1.36e-2	13.3768	0.7057	0.6637
8	0.000231358	1.151037266	3.21331E-06	18416	4.352e-3	2.307e-2	17.67421	0.7495	0.8004
9	0.000256527	1.27625471	3.56288E-06	20419.2	5.21e-3	3.025e-2	27.36814	0.6678	0.8049
10	0.00027642	1.375224868	3.83917E-06	22003.2	5.9505e-3	3.6885e-2	37.7191	0.6130	0.82
11	8.38141E-05	0.416985476	1.16408E-06	6670.4	7.3786e-4	1.61e-3	2.34602	0.7453	0.765
12	9.73175E-05	0.484166469	1.35163E-06	7745.6	9.5786e-4	2.38e-3	3.147181	0.7471	0.6115
13	0.000133894	0.666138623	1.85964E-06	10657.6	1.670e-3	5.486e-3	5.94225	0.7481	0.801
14	8.56285E-05	0.426012396	1.18928E-06	6816	7.646e-4	1.699e-3	2.434624	0.7474	0.586
15	0.000111473	0.554590683	1.54823E-06	8872	1.213e-3	3.3979e-3	4.132407	0.7469	0.6557

Chapter 5

Conclusion

In this project, simulation of turbulent flow through an orifice meter was done using κ -ϵ RANS turbulence model.The coefficient of discharge was determined for 15 different cases and Reynolds number in the range of 6000-20000. The obtained discharge coefficient was compared with experimentally obtained values. Velocity and pressure contours and streamlines were visualised through which various distinctive flow behaviours were studied.

Part II

Case Study 2: Flow through sudden expansion and contraction

Chapter 6

Introduction

6.1 Aim

The aim of this case study was to determine the minor loss factor of sudden expansion and contraction of pipes through CFD method. OpenFOAM version 1912 was used for carrying out the simulation. Further, the velocity and pressure contours of the flow were studied. The study was performed for a 2-D incompressible flow with water as the working fluid, simpleFoam steady state solver was used and κ-ϵ RANS model was adopted to simulate the turbulent flow. The results were viewed in ParaView 5.7.0

6.2 Theory

The resistance to flow in a pipe network causes loss in the pressure head along the flow. The overall head loss across a pipe network consists of the following:

- Major losses
- Minor losses

6.2.1 Major Losses

Major losses refer to the losses in pressure head of the flow due to friction effects. Such losses can be evaluated by using the Darcy-Weisbach equation:

$$h_{major} = f\frac{Lv^2}{2gD} \tag{6.1}$$

where f is the Darcy friction factor, L is the length of the pipe segment, v is the flow velocity, D is the diameter of the pipe segment, and g is acceleration due to gravity. Equation 6.1 is valid for any fully developed, steady and incompressible flow. The friction factor f can be calculated by the following empirical formula, known as the Blasius formula, valid for turbulent flow in smooth pipes with $Re_D < 10^5$:

$$f = 0.316 Re_D^{-0.25} \tag{6.2}$$

6.2.2 Minor Losses

In a pipe network, the presence of pipe fittings such as bends, elbows, valves, sudden expansion or contraction causes localized loss in pressure head. Such losses are termed as minor losses. Minor losses are expressed using the following equation:

$$h_{minor} = K\frac{v^2}{2g} \tag{6.3}$$

where K is called the Loss Coefficient of the pipe fitting under consideration. Minor losses are also expressed in terms of the equivalent length of a straight pipe (L_{eq}) that would cause the same head loss as the fitting under consideration:

$$h_{minor} = K\frac{v^2}{2g} = f\frac{L_{eq}v^2}{2gD} \tag{6.4}$$

$$L_{eq} = K\frac{D}{f} \tag{6.5}$$

In the present study, we shall determine the head losses across sudden enlargement and sudden contraction. Loss of head due to sudden enlargement: This is the energy loss due to sudden enlargement. Sudden enlargement in the diameter of pipe results in the formation of eddies in the flow at the corners of the enlarged pipe 6.1. This results in the loss of head across the fitting. Loss of head due to sudden contraction: This is the energy loss due to sudden contraction. In reality, the head loss does not take place due to the sudden contraction but due to the sudden enlargement, which takes place just after vena-contracta 6.2.[4][5] Figure 6.3 shows the schematic layout of the pipe network to be used in the present study.

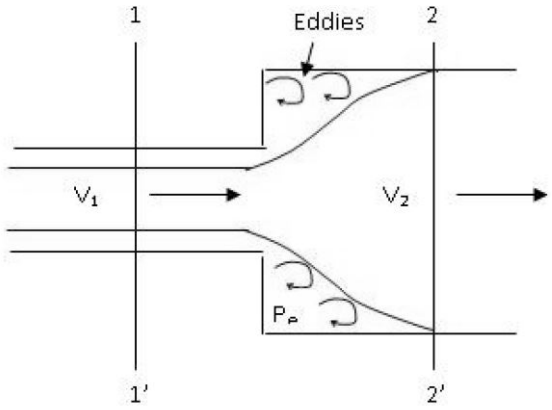

Figure 6.1: Sudden Expansion[3]

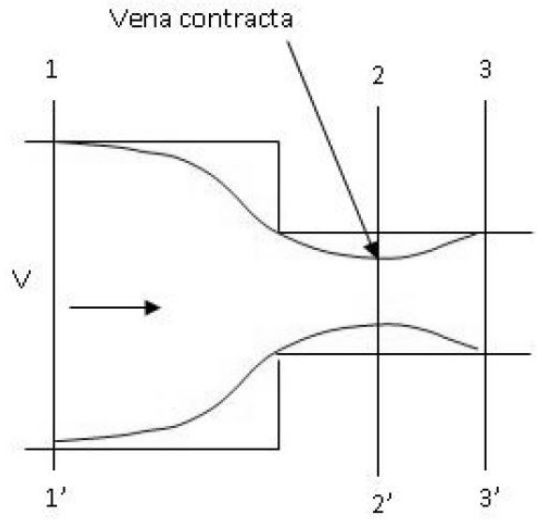

Figure 6.2: Sudden Contraction[3]

6.3 Problem Statement

The primary objective of the case study is to simulate turbulent flow through a sudden expansion and contraction case and later calculate the minor loss factors using the CFD result and compare it with the experimental or analytical results. The dimensions of the pipe fittings are considered from the lab manual. The simulations were conducted for 17 different cases with reynolds number varying from the range of 6000 to 20000. To study this turbulent flow, simpleFoam solver is used.

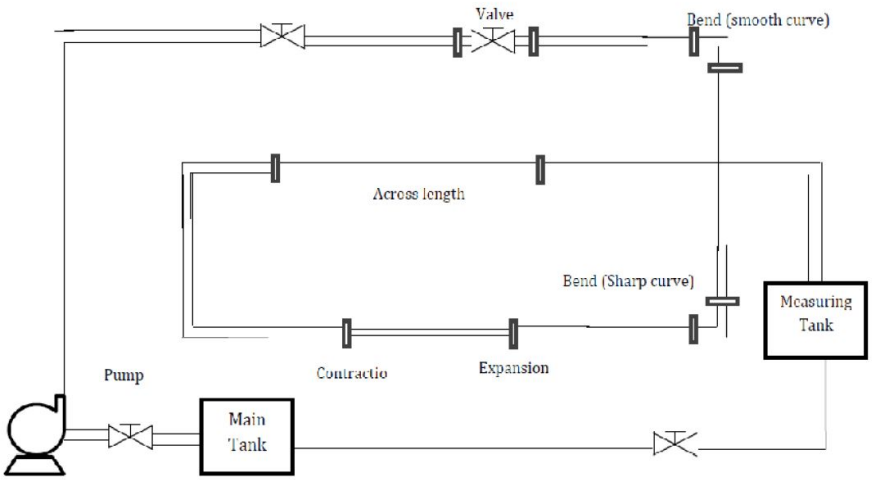

Figure 6.3: Schematic layout of pipe network with fittings[3]

6.4 Schematic Diagram

The dimensions of the geometry is given below
Diameter of the collecting tank, D_c = 0.28 m
Diameter of the larger cross-section pipe, D_1 = 14.3 mm
Diameter of the smaller cross-section pipe, D_2 = 9.22 mm
The geometry of the sudden expansion and contraction case is shown in the Figure 6.4 and Figure 6.5 respectively.

Figure 6.4: Axisymmetric Geometry of sudden expansion

Figure 6.5: Axisymmetric Geometry of sudden contraction

Chapter 7

OpenFOAM base case

7.1 pitzDaily

The base case considered for the simulation of the orifice meter is the pitzDaily case. This case can be found under the incomressible section, simpleFoam subsection. The directory for this is
\OpenFOAM-v1912\tutorials\incompressible\simpleFoam\pitzDaily.
Based on the experimental work of Pitz and Daily (1981). It features a backward facing step. Such a "classic" case is instructive for comparing different turbulence models with respect to the size and shape of the recirculation zone[internet reference]. pitzDaily introduces the dollowing concepts for the first time:

- Mesh creation using blockMesh and also mesh grading capability
- Turbulent steady flow.

7.1.1 Folder Structure

Any case file in OpenFOAM has three folders, called the 0, constant and the system. The constant contains coefficient values that will be used in equations and also things which will remain constant like the mesh, material properties, environmental constants which the solver uses, the 0 folder contains the initial and boundary conditions, and the system folder contains the configuration files for the mesh and also how the solver will be executed, schemes and methods to use and controls for the simulation.

Table 7.1: Folder contents

Directories	Constant	0	System
Sub-directories	transportProperties turbulenceProperties polyMesh	U p nut epsilon k	blockMeshDict fvSchemes fvSolution

7.2 Solver

OpenFOAM or Open-source Field Operation And Manipulation is an open-source C++ tool used for solving continuum mechanics problems, with a focus on Finite Volume Method (FVM). The software package includes solver codes for different kinds of transport phenomena, varying from simple laplacian solver called laplacianFoam to complex multiphase flow, compressible flow, heat transfer, incompressible flow, and many more. The flagship solver and most commonly used solver is simpleFoam. simpleFoam is a steady-state solver for incompressible, turbulent flow. It utilizes the SIMPLE (Semi-Implicit Method for Pressure Linked Equations) algorithm. It is an approximation of the velocity field which is obtained by solving the momentum equation. The pressure gradient term is calculated using the pressure distribution from the previous iteration or an initial guess. The pressure equation is formulated and solved to obtain the new pressure distribution. Velocities are corrected and a new set of conservative fluxes is calculated. The solver used for this case study is simpleFoam, it employs SIMPLE algorithm. The case study considered is a steady state, incompressible, three-dimensional flow. The set of Navier Stokes equations governing the flow is given below.
The continuity equation is given as,

$$\nabla.\vec{u} = 0 \tag{7.1}$$

The momentum equation is given as.

$$\frac{\partial \vec{u}}{\partial t} + \nabla.[\vec{u}\vec{u}] = -\frac{1}{\rho}\nabla p + \nu\nabla^2\vec{u} \tag{7.2}$$

Where, $\vec{u}$ is velocity, p-pressure; ν is kinematic viscosity The discretized momentum equation and pressure correction equation are solved implicitly, where the

velocity correction is solved explicitly. This is the reason why it is called "Semi-Implicit Method".

7.2.1 Turbulence Model

The turbulence model considered for the simulation is κ -ϵ RANS model. κ -ϵ model solves two additional equations, for turbulent kinematic energy κ and rate of dissipation of turbulence energy ϵ It performs poorly for complex flows involving severe pressure gradient, separation, strong streamline curvature. Suitable for initial iterations, initial screening of alternative designs, and parametric studies. Can be only used with wall functions. The equations for the κ -ϵ RANS model is below,

$$\frac{\partial(p\kappa)}{\partial t} + \frac{\partial(p\kappa u_i)}{\partial x_i} = \frac{\partial}{\partial x_j}[\frac{\mu_t}{\sigma_\kappa}\frac{\partial \kappa}{\partial x_j}] + 2\mu_t E_{ij}E_{ij} - \rho\epsilon \tag{7.3}$$

$$\frac{\partial(p\epsilon)}{\partial t} + \frac{\partial(p\epsilon u_i)}{\partial x_i} = \frac{\partial}{\partial x_j}[\frac{\mu_t}{\sigma_\kappa}\frac{\partial \kappa}{\partial x_j}] + C_{1\epsilon}\frac{\epsilon}{\kappa}2\mu_t E_{ij}E_{ij} - C_{2\epsilon}\rho\frac{\epsilon^2}{\kappa} \tag{7.4}$$

where u_i represents velocity component in corresponding direction, E_{ij} represents component of rate of deformation, and μ_t represents eddy viscosity. The default value of model coefficients [6]: $C_{1\epsilon}$, $C_{2\epsilon}$, σ_κ, σ_ϵ and $C\mu$ have been used.

Chapter 8

OpenFOAM Case Modifications

Using the pitzDaily case, modifications were made with the geometry, the mesh used, boundary conditions applied to it, and the control parameters which are going to be explained further in the below sections.

8.1 Pre-processing

The models for both the case was created using the dimensions from the manual provided [3]. To simplify the calculations, an axisymmetric wedge was created. In OpenFOAM to make the axisymmetric wedge the angle should be 5 degrees. The upstream length and downstream length was taken to be 400mm and axis along Z direction for both the cases.
The mesh and geometry was created using the blockMesh utility. The blockMeshDict file from the base case was modified to create the axisymmetric model of the sudden expansion and contraction geometry. convertToMeters, the very first line of blockMeshDict file was changed, by default the units used in OpenFOAM are in meters. Since the geometry is in millimetres a conversion factor from meters to millimetres was used, replacing 0.01 to 0.001.
The co-ordinates of the geometry are entered in the vertices column of the file. It is entered as x, y, and z coordinate values. X represents the radial distance; Y represents the angular axis and Z represents the axial length of the geometry for sudden expansion case and Y represents the radial distance; X represents the angular axis and Z represents the axial length of the geometry for sudden contraction case. Therefore the coordinate axis can be obtained by simple trigonometric formula

of $tan = \frac{Oppositeside}{adjacentside}$. The geometry is divided into blocks for Meshing purposes. There are totally 3 blocks. It was made using hexahedral blocks with simplegrading 1 in all directions to make sure the nearest cell thickness near the wall region would be in the log-law region for sudden expansion case and for the sudden contraction case, the expansion ratio was chosen (0.015), to have refinement near the walls so that the nearest cell thickness near the wall region would be in the viscous sub-layer region. In the axisymmetric geometry, the front, back panels, and the axis are additional boundaries. Proper patchfields are assigned to them, for the front and back panels, boundary patch assigned is wedge and for the axis it is given as empty. Using the blockMesh utility, the mesh was generated and with checkMesh, the quality of the mesh was determined. For the sudden expansion case, the y+ value was selected in the log-law region as suggested in [9] and for sudden contraction the y+ was considered in the viscous sublayer.

8.2 Boundary conditions

The initial and boundary conditions are included in the 0 folder as k, epsilon, nut,p, and U. The boundary conditions are summarised in the Table 8.1 for both the cases. In all the files in 0 folder, the axis, front_back_pos and front_back_neg were given

Table 8.1: Boundary conditions

	inlet	outlet	wall
epsilon	fixedValue	zeroGradient	epsilonWallFunction
k	fixedValue	zeroGradient	kqRWallFunction
nut	calculated	calculated	nutkWallFunction
p	zeroGradient	fixedValue	zeroGradient
U	fixedValue	zeroGradient	noSlip

the boundary condition of empty, wedge and wedge respectively. The value for κ and ϵ were determined using the below equations

$$\kappa = \frac{3}{2}(uI)^2 \tag{8.1}$$

$$\epsilon = \frac{C_\mu^{0.75}\kappa^{1.5}}{0.07l} \tag{8.2}$$

where u is the free stream velocity, I is the turbulence intensity, C_μ is the model coefficient, l is the characteristic length.

8.3 Physical properties

The working fluid for both the simulation was water. The density considered was 1000 kg/ m^3, with a kinematic viscosity of 1×10^{-06} $m^2/\ s$. So the value in the transportProperties file was changed to 1×10^{-06} from 1×10^{-05} and the transportModel remained as it is to Newtonian.

8.4 fvSchemes & fvSolution

fvSchems and fvSolutions are found under the constant folder. fvSolution directory contains equation solvers, algorithms and tolerances. No changes were done to this file, the tolerances for the residuals were pre-set to a value of 1e-05 and it was not changed. The numerical schemes for the simulation are entered in the fvSchemes dictionary. No changes were made in this file directory.

8.5 Control parameters

The OpenFOAM solvers begin all runs by setting up a database. The database controls I/O and, since output of data is usually requested at intervals of time during the run, time is an inextricable part of the database. The controlDict dictionary sets input parameters essential for the creation of the database. Here the endTime was changed to 10000, i.e., maximum iterations were 10000. startTime was 0 and writeInterval was set to every 100 iterations with 1 as deltaT as it was a steady state analysis.

8.6 Post-processing

After the simulation has been completed, the results were viewed in ParaView. To do this, first the results obtained were converted into viewable file using the command *touch suitable_file_name.foam*. A file with .foam extension was created. In this file, the results was viewed, the various contours of the solution was visualised,

streamlines were plotted and the data were analysed with the in-built plotting options available.

Chapter 9

Results

Steady state simulations were performed using SIMPLE algorithm for κ -ϵ RANS model. The obtained CFD results have been compared with the experimental results for the coefficient of discharge. Post-processing was done using paraview.

9.1 Numerical Results

The post-processing of the simulation was done in ParaView for both the cases each having 17 simulations. The numerical results are further discussed below.

9.1.1 Sudden Expansion

The velocity and pressure contours obtained by the simulations are shown in Figure 9.1 and 9.2. From the pressure contour we can see that there is a gradual decrease in pressure due to the frictional losses at the inlet.

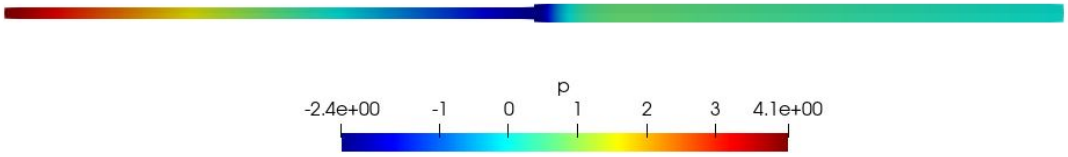

Figure 9.1: Pressure contour

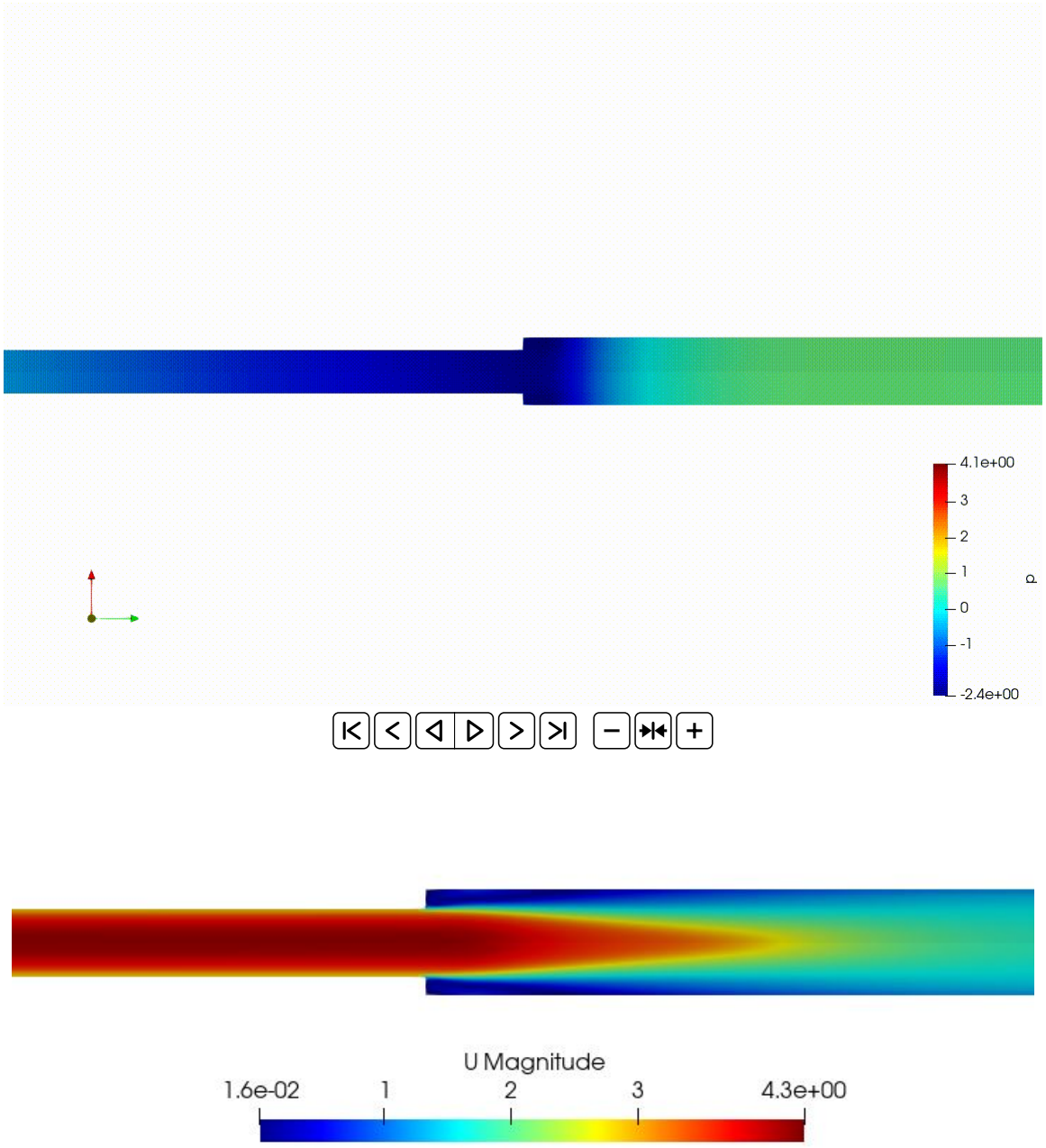

Figure 9.2: Velocity contour

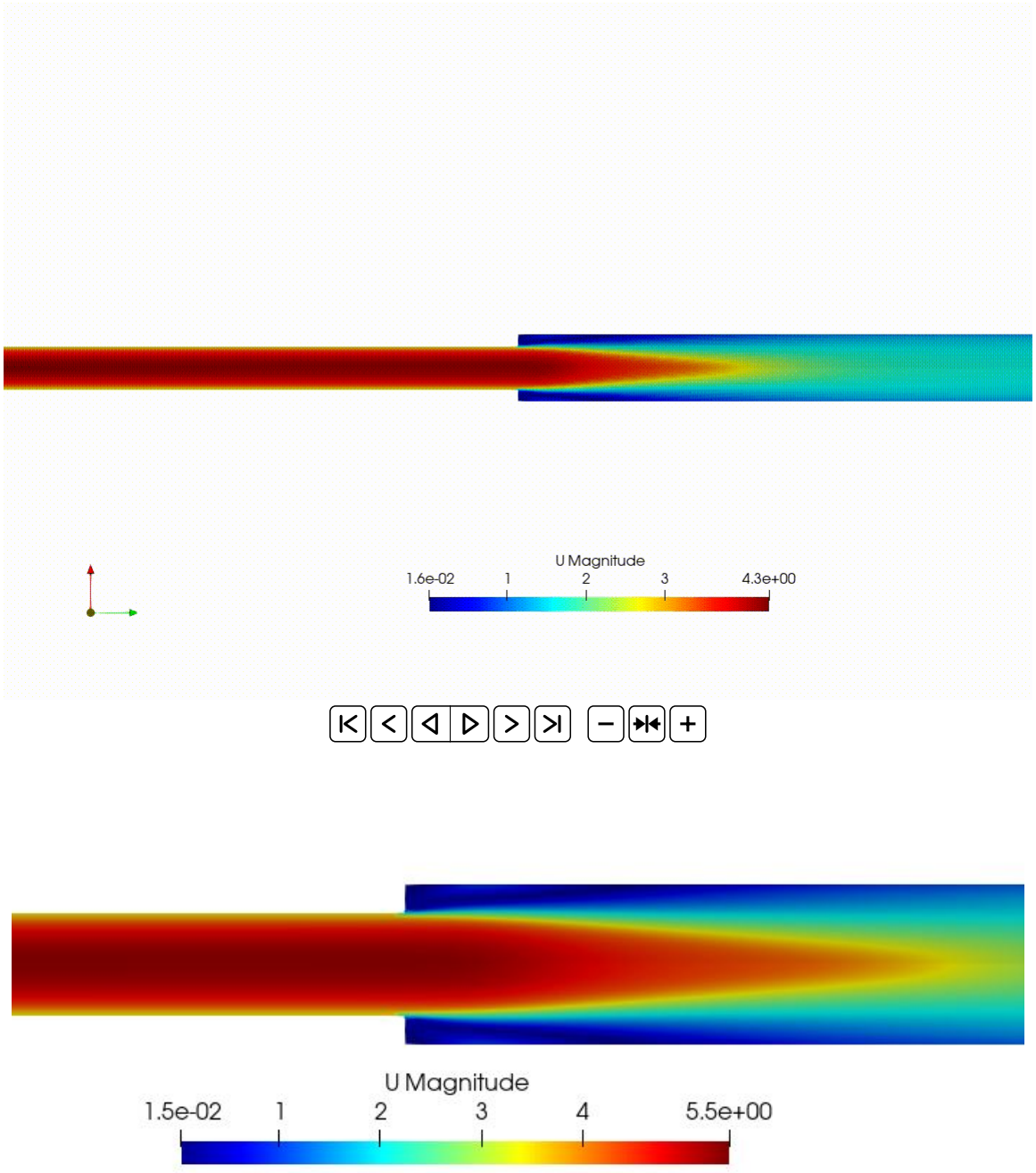

Figure 9.3: Velocity contour for higher Reynolds number

As the fluid reaches the transitional section, the fluid is decelerated in the enlarged pipe area and there occurs a sudden rise in pressure[10]. In the velocity contour it is seen that right after the transitional region, eddies are formed. The evolution

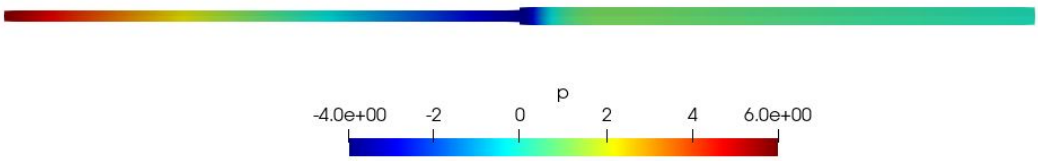

Figure 9.4: Pressure contour for higher Reynolds number

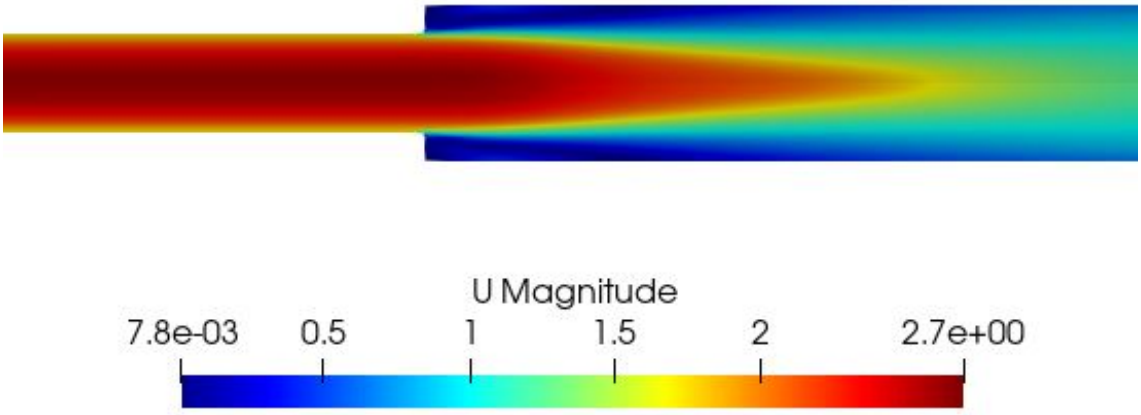

Figure 9.5: Velocity contour for lower Reynolds number

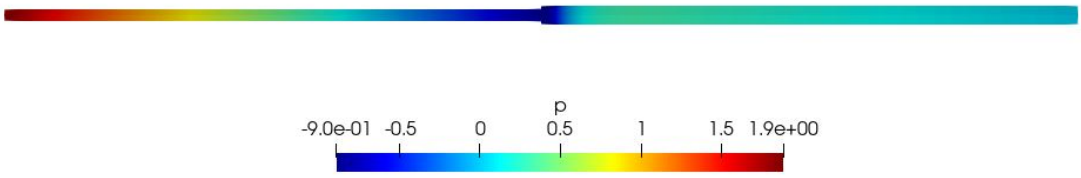

Figure 9.6: Pressure contour for lower Reynolds number

of the solution is plotted for both pressure and velocity. Furthermore, pressure and velocity contours for lower and higher Reynolds number are plotted which

are shown in Figure 9.3-9.6. This can be further visualised through the streamlines plotted for this case as shown in Figure 9.7 The re-circulation region right

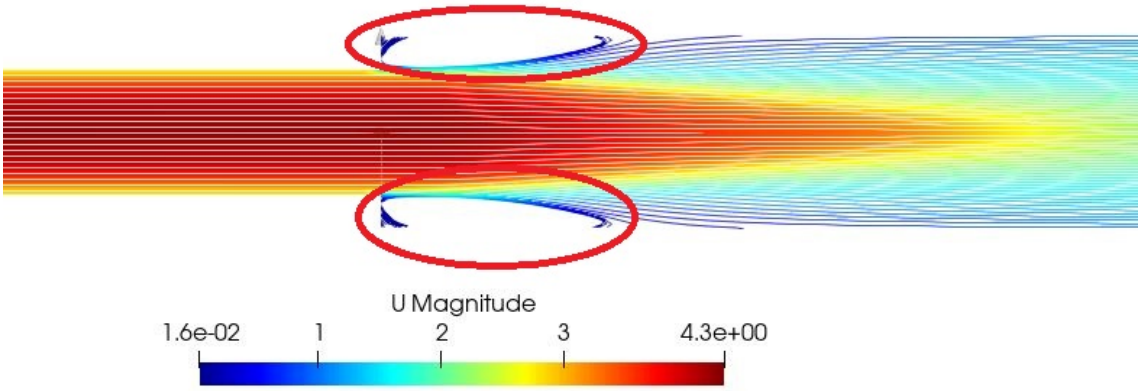

Figure 9.7: Streamlines with Velocity contour

after the expansion can be seen in the streamline. Re-circulation region is circled in red colour Streamlines for higher and lower Reynolds number are also plotted and is shown in Figure 9.8 and Figure 9.9 respectively. Pressure and velocity distribution along the length of the pipe is plotted as shown in Figure 9.10 and Figure 9.11. From these graphs we see that right after the change in cross-sectional are, there is a sudden increase in the pressure and drop in the velocity around the length of 0.4-0.45m. The pressure change at the expansion plane (ΔP_e) is obtained by extrapolating the computed pressure profiles upstream and downstream of the pipe expansion (in the region of fully developed pipe flow) to the expansion plane. Vector plots for the different Reynolds number is shown in Figure 9.12-9.14.

9.1.2 Sudden Contraction

Contours for pressure and velocity are shown in Figure 9.15 and Figure 9.16. From the pressure contour it can be seen that at a few distance from the entrance of the sudden contraction, there is a high pressure region and after the change in geometry, the pressure value decreases suddenly and then gradually to zero. In the

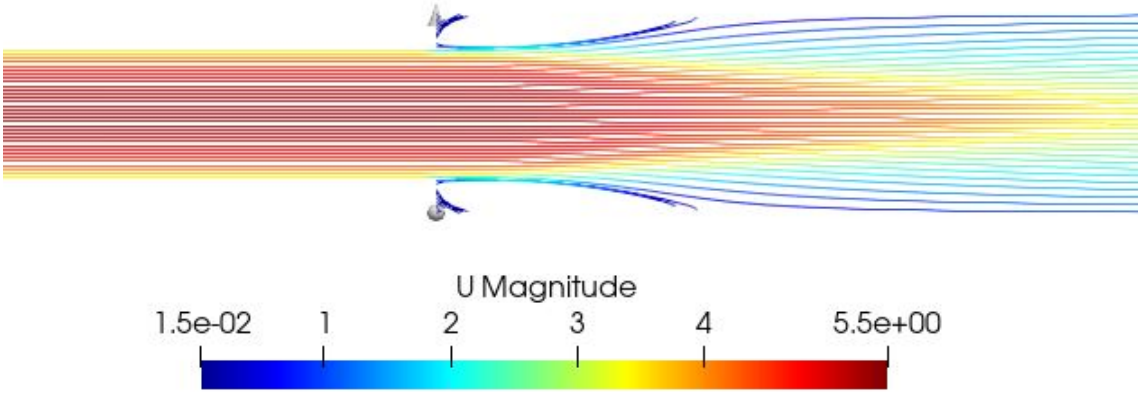

Figure 9.8: Streamlines with Velocity contour for Higher Reynolds number

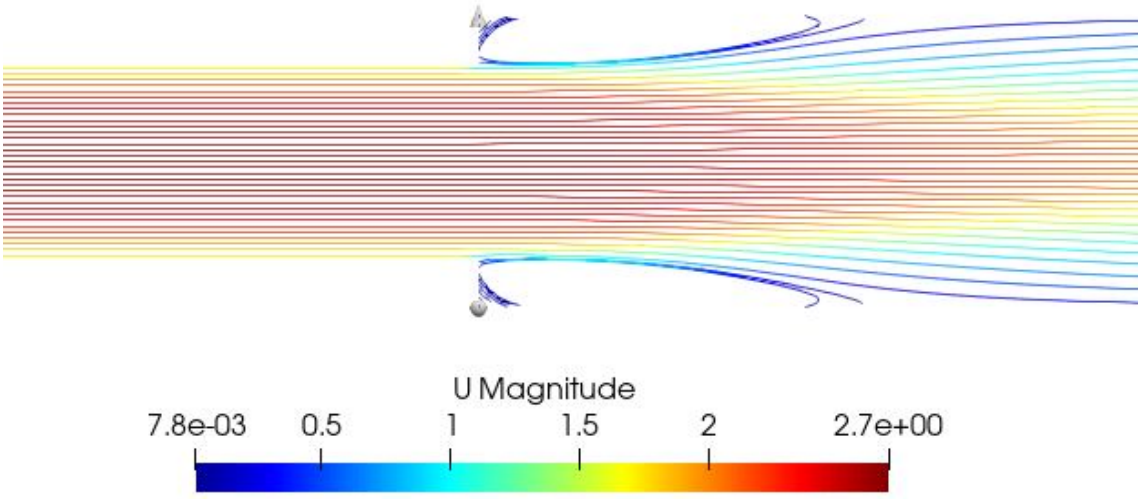

Figure 9.9: Streamlines with Velocity contour for Lower Reynolds number

velocity contour, the magnitude of the velocity is low before the sudden contraction is approached, at the entrance there's an increase in the velocity and after the

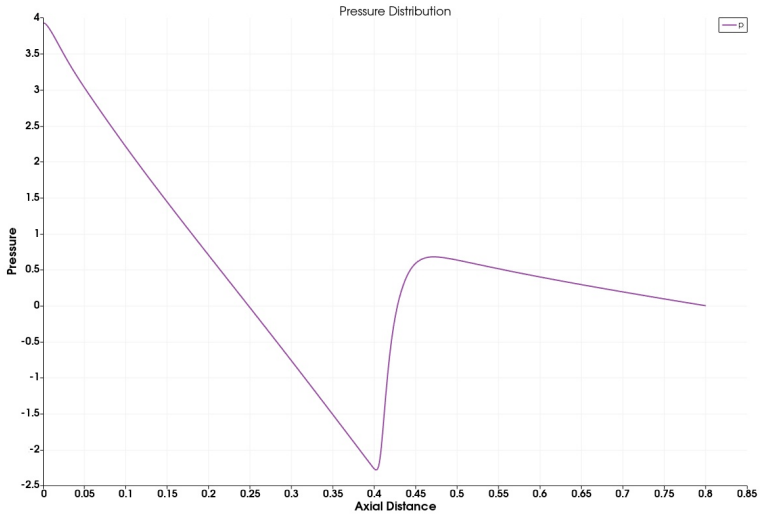

Figure 9.10: Pressure Distribution along the length

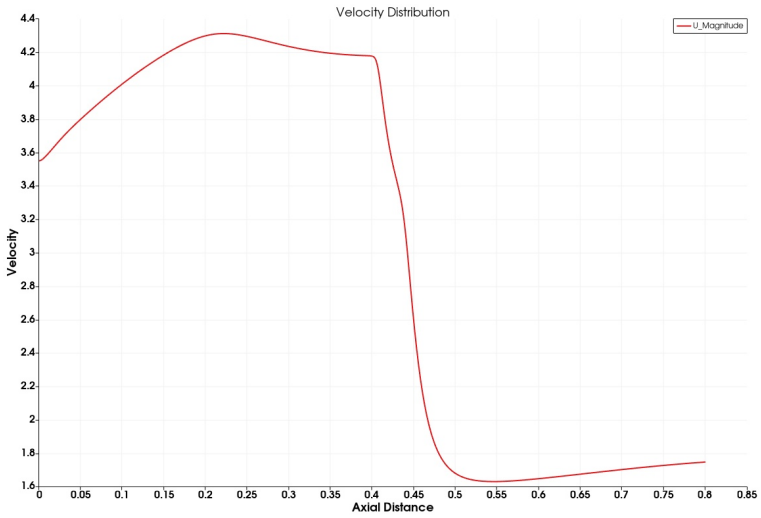

Figure 9.11: Velocity Distribution along the length

change in geometry, the value saturates. Velocity and pressure contours for higher and lower Reynolds number are also plotted to get a better understanding of the flow for various Reynolds number regime and is shown in Figure 9.17-9.20
To better understand the flow, streamlines were plotted and is shown in Figure 9.21 From these streamlines we can see, the fluid converges before the entrance and a region of vena-contracta is forming few metres right after the entrance. Streamlines are also plotted for higher and lower Reynolds number, as shown in Figure 9.22 and 9.23. Pressure and velocity distributions were plotted along the length

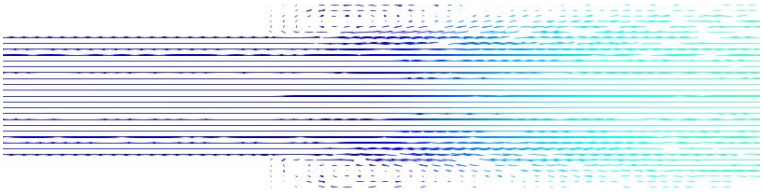

Figure 9.12: Vector plot for sudden expansion

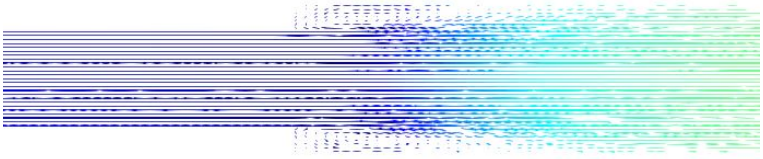

Figure 9.13: Vector plot for sudden expansion (High Reynolds number)

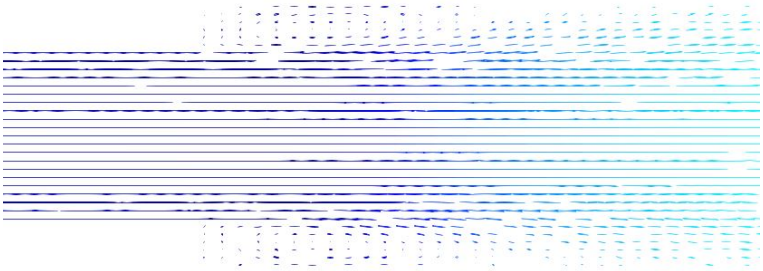

Figure 9.14: Vector plot for sudden expansion (Low Reynolds number)

of the pipe and is shown in Figure 9.24 and Figure 9.25. The plots obtained show the same physics that was seen in the pressure and velocity contours. Vector plots have also been plotted to get a better understanding for various Reynolds number. They are shown in Figure 9.26-9.28.

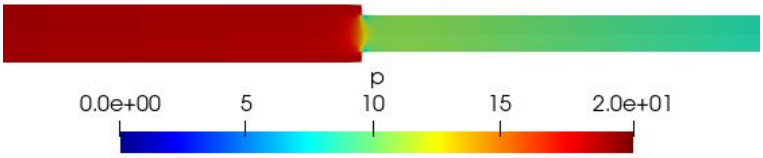

Figure 9.15: Pressure contour

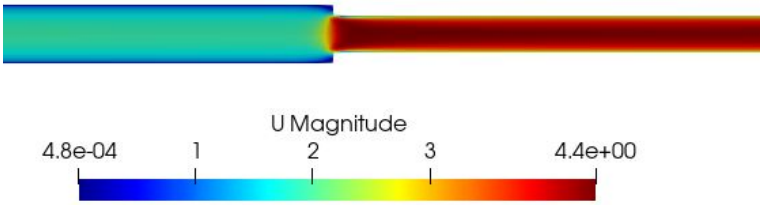

Figure 9.16: Velocity contour

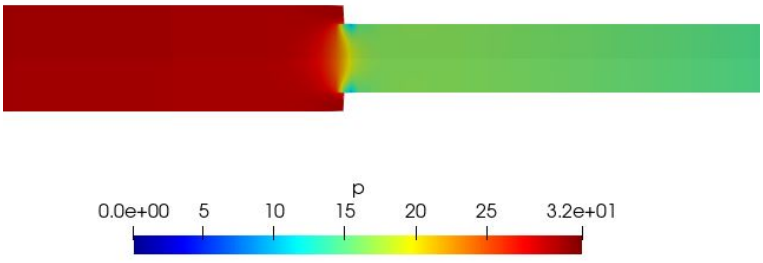

Figure 9.17: Pressure contour for Higher Reynolds number

9.2 Experimental Results

The experimental data was provided in the manual [3]. The initial and final height of the collecting tank and the manometer's height difference was given. Using the

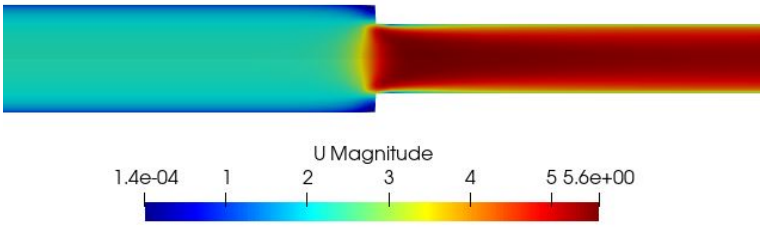

Figure 9.18: Velocity contour for Higher Reynolds number

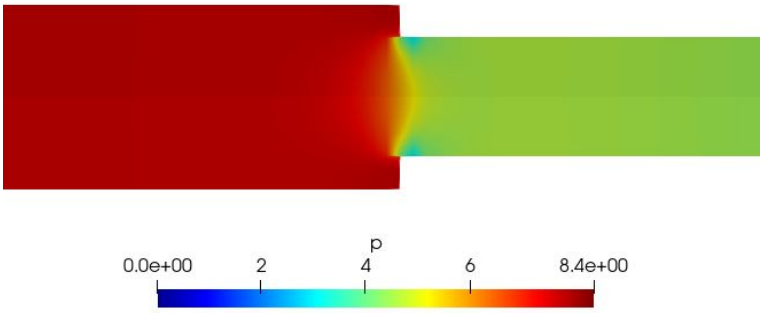

Figure 9.19: Pressure contour for Lower Reynolds number

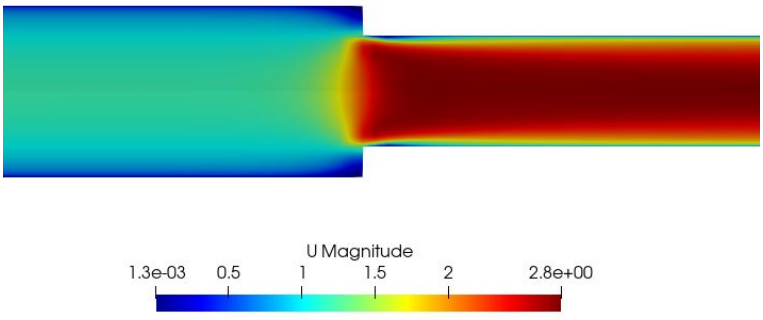

Figure 9.20: Velocity contour for Lower Reynolds number

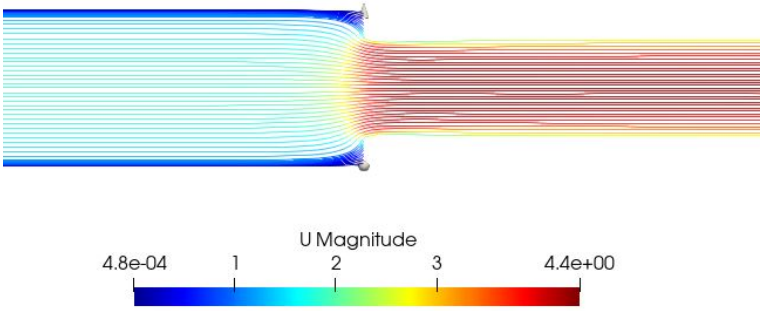

Figure 9.21: Streamlines with Velocity contour

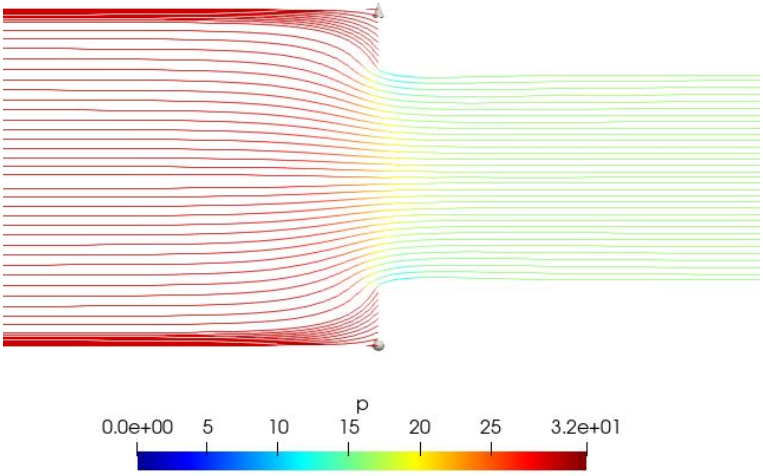

Figure 9.22: Streamlines with Velocity contour for Higher Reynolds number

collecting tanks reading, the flow rate was determined and the pressure head was determined using manometer's height difference. With Equation 6.3, the minor loss factor K for the experiment data was determined.

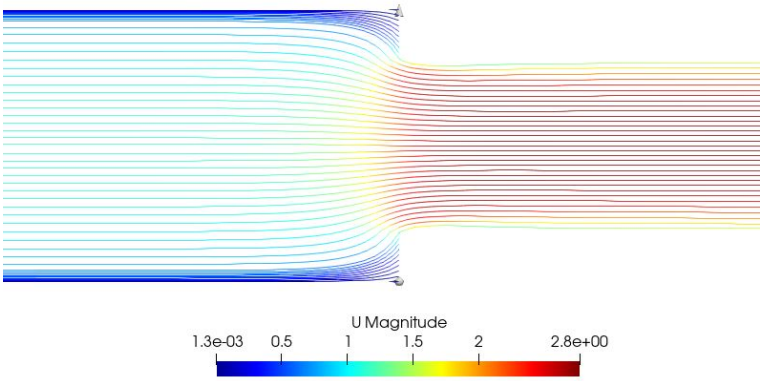

Figure 9.23: Streamlines with Velocity contour for Lower Reynolds number

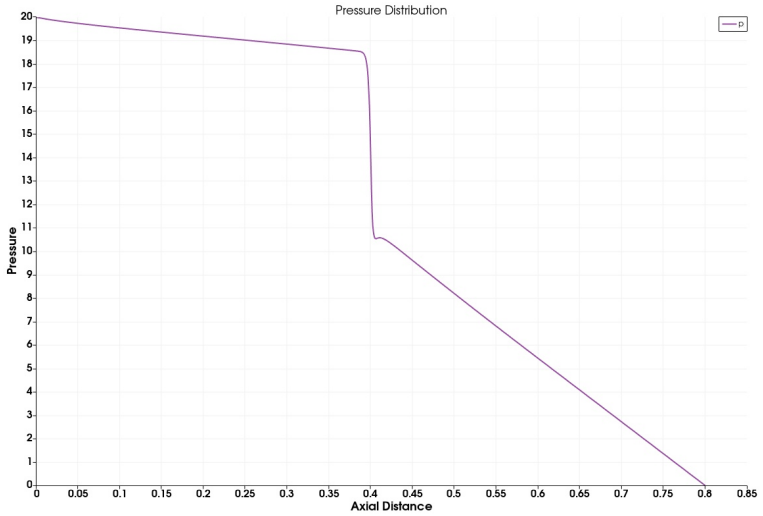

Figure 9.24: Pressure Distribution along the length

9.3 Result comparison

9.3.1 Sudden Expansion

The theoretical value for sudden expansion geometry was determined using the equation 9.1 and was determined to be equal to 0.3414.

$$K_{se} = (1 - \frac{d^2}{D^2})^2 \tag{9.1}$$

Both the results obtained, CFD and experimental were compared and is summarised in the Table 9.1 with the input initial conditions for CFD simulations.

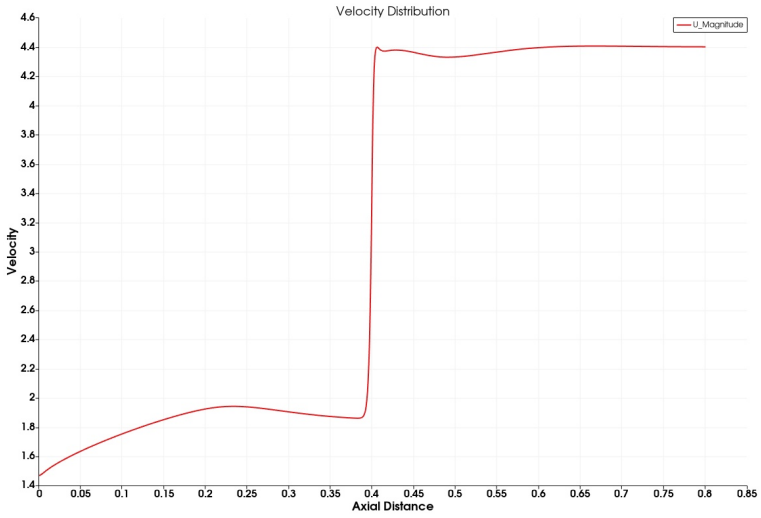

Figure 9.25: Velocity Distribution along the length

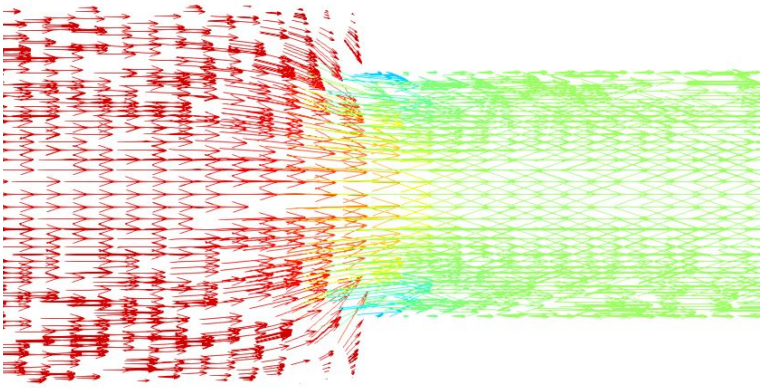

Figure 9.26: Vector plot for sudden contraction

9.3.2 Sudden Contraction

The analytical result for the given sudden contraction geometry was determined using the below equation,

$$K_{sc} = 0.42(1 - \frac{d^2}{D^2}) \tag{9.2}$$

Minor loss factor was determined only for the CFD simulations, as the loss factor from the experimental data gave a value greater than one. The values obtained are summarised in Table 9.2

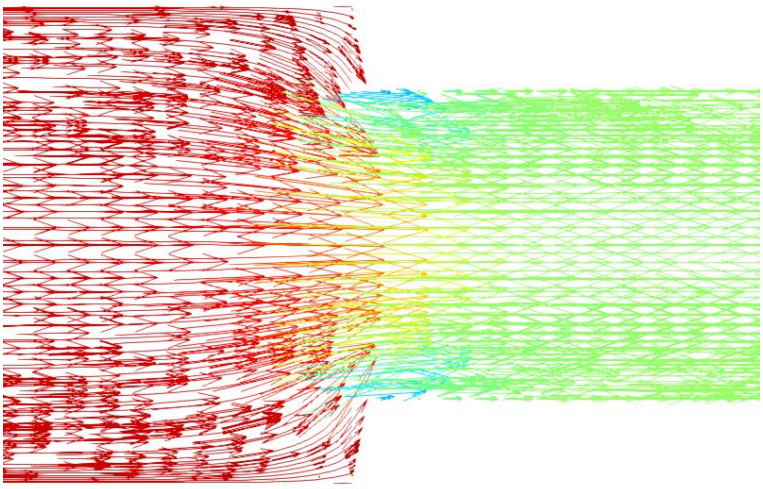

Figure 9.27: Vector plot for sudden contraction (High Reynolds number)

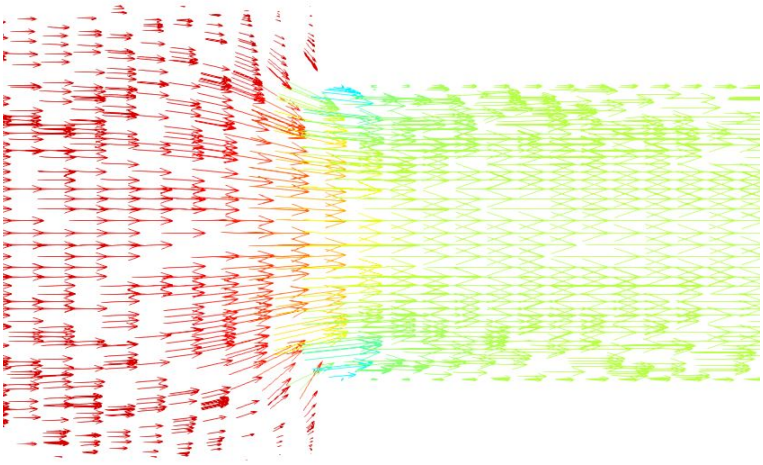

Figure 9.28: Vector plot for sudden contraction (Low Reynolds number)

Table 9.1: Experimental and CFD results for sudden expansion

Sl No.	Flow rate(m^3/s)	Velocity (m/s)	Reynolds number	Turbulent kinetic energy (m^2/s^2)	Turbulent dissipation (m^2/s^3)	Pressure difference	K	K (exp)
1	0.000237261	3.553680534	32731	0.035935	1.7343	2.9593	0.4696	0.57622
2	0.000235939	3.533868651	32546.6	0.03553	1.7050	2.926	0.4686	0.638518
3	0.000202062	3.026465624	27903.408	0.027205	1.142	2.1416	0.4696	0.795926
4	0.0002099	3.143867317	28985.83	0.0289631	1.2508	2.3152	0.4696	0.569403
5	0.000194248	2.909425024	26824.668	0.025362	1.0283	1.9748	0.4696	0.607656
6	0.000181724	2.721851542	25078.4	0.022572	0.8632	1.7373	0.4696	0.444568
7	0.000300587	4.502156972	41490	0.0544	3.2303	4.7817	0.4722	0.646404
8	0.000293977	4.403161169	40568	0.0523	3.0451	4.5716	0.4722	0.637544
9	0.000282542	4.231889663	39000	0.04199	2.1906	4.2252	0.4722	0.717801
10	0.000277277	4.153026675	38263	0.04728	2.6173	4.0669	0.4722	0.630656
11	0.000287787	4.31044135	39738.2	0.05052	2.8909	4.3865	0.4722	0.705183
12	0.000290918	4.3573383	40107	0.05134	2.9616	4.4683	0.4722	0.390614
13	0.000104913	1.571377203	14475.4	0.008629	0.204	0.5788	0.4696	0.500586
14	0.000146918	2.200528707	20284	0.01557	0.4946	1.1365	0.4696	0.32163
15	9.87793E-05	1.479507415	13553.4	0.00769	0.1716	0.5074	0.4696	0.498051
16	0.000105852	1.585441164	14567.6	0.008725	0.2075	0.5862	0.4696	0.185879
17	6.28834E-05	0.941862287	8666.8	0.003516	0.053	0.2051	0.4642	0.351128

Table 9.2: Experimental and CFD results for sudden expansion

Sl No.	Flow rate(m^3/s)	Velocity (m/s)	Reynolds number	Turbulent kinetic energy (m^2/s^2)	Turbulent dissipation (m^2/s^3)	Pressure difference	K
1	0.000237	1.478038	21021	0.006858	0.09322	0.3024	0.2799
2	0.000236	1.469798	20878	0.0068	0.0922	0.2721	0.2553
3	0.000202	1.25876	17875	0.00518	0.0613	0.142	0.18176
4	0.00021	1.307589	18590	0.00555	0.068	0.2244	0.2656
5	0.000194	1.210081	17303	4.901e-3	0.0563	0.1056	0.1442
6	0.000182	1.132066	16159	4.348e-3	0.047	0.1576	0.2469
7	0.000301	1.872526	26741	0.0105	0.1766	0.5019	0.287
8	0.000294	1.831351	26169	0.0101	0.166	0.4884	0.2916
9	0.000283	1.760117	25168	9.4437e-3	0.1506	0.4663	0.301
10	0.000277	1.727316	24596	9.071e-3	0.1418	0.4468	0.3020
11	0.000288	1.792788	25597	9.727e-3	0.1574	0.4898	0.3057
12	0.000291	1.812293	25883	9.918e-3	0.1621	0.4812	0.2937
13	0.000105	0.653563	9345.05	1.65e-3	0.011	0.0604	0.286
14	0.000147	0.915238	13013	2.9772e-3	0.0266	0.1158	0.2799
15	9.88E-05	0.615353	8723	1.4785e-3	9.3321e-3	0.04411	0.237
16	0.000106	0.659413	9295	1.6523e-3	0.011	0.0547	0.2593
17	6.29E-05	0.391737	5577	6.7586e-4	2.8842e-3	0.01096	0.1442

Chapter 10

Conclusion

In this case study, simulation of turbulent flow through sudden exapnsion and contraction was done using κ -ϵ RANS turbulence model.The minor loss factor was determined for both the cases in Reynolds number range of 5500-40000. The obtained minor loss factor was compared with theoretical and experimentally obtained values. Velocity, pressure contours and streamlines were visualised through which various distinctive flow behaviours were studied.

Part III

Case Study 3: Flow through smooth and sharp bends

Chapter 11

Introduction

11.1 Aim

The aim of this case study was to determine the minor loss factor of smooth and sharp bend of pipes through CFD method. OpenFOAM version 1912 was used for carrying out the simulation. Further, the velocity and pressure contours of the flow were studied. The study was performed for a 3-D incompressible flow with water as the working fluid, simpleFoam steady state solver was used and κ-ω SST RANS model was adopted to simulate the turbulent flow. The results were viewed in ParaView 5.7.0

11.2 Theory

The resistance to flow in a pipe network causes loss in the pressure head along the flow. The overall head loss across a pipe network consists of the following:

- Major losses
- Minor losses

11.2.1 Major Losses

Major losses refer to the losses in pressure head of the flow due to friction effects. Such losses can be evaluated by using the Darcy-Weisbach equation:

$$h_{major} = f\frac{Lv^2}{2gD} \tag{11.1}$$

where f is the Darcy friction factor, L is the length of the pipe segment, v is the flow velocity, D is the diameter of the pipe segment, and g is acceleration due to gravity. Equation 11.1 is valid for any fully developed, steady and incompressible flow. The friction factor f can be calculated by the following empirical formula, known as the Blasius formula, valid for turbulent flow in smooth pipes with $Re_D < 10^5$:

$$f = 0.316 Re_D^{-0.25} \tag{11.2}$$

11.2.2 Minor Losses

In a pipe network, the presence of pipe fittings such as bends, elbows, valves, sudden expansion or contraction causes localized loss in pressure head. Such losses are termed as minor losses. Minor losses are expressed using the following equation:

$$h_{minor} = K\frac{v^2}{2g} \tag{11.3}$$

where K is called the Loss Coefficient of the pipe fitting under consideration. Minor losses are also expressed in terms of the equivalent length of a straight pipe (L_{eq}) that would cause the same head loss as the fitting under consideration:

$$h_{minor} = K\frac{v^2}{2g} = f\frac{L_{eq}v^2}{2gD} \tag{11.4}$$

$$L_{eq} = K\frac{D}{f} \tag{11.5}$$

In the present study, we shall determine the head losses across smooth and sharp bend. Loss of head due to bend in pipe: This is the energy loss due to bend. When a bend is provided in the pipeline, there is a change in direction of the velocity of flow Figure 11.1 and 11.2. Due to this, the flow separates from the walls of the bend and formation of eddies takes place. Figure 11.3 shows the schematic layout of the pipe network to be used in the present study.

11.3 Problem Statement

The primary objective of the case study is to simulate turbulent flow through a sharp and smooth bend case and later calculate the minor loss factors using the

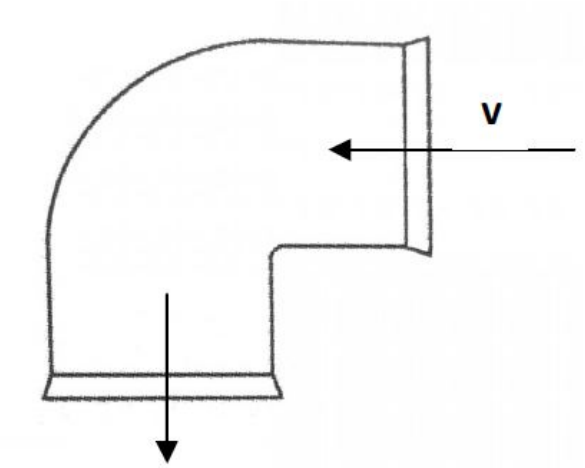

Figure 11.1: Sharp Bend[3]

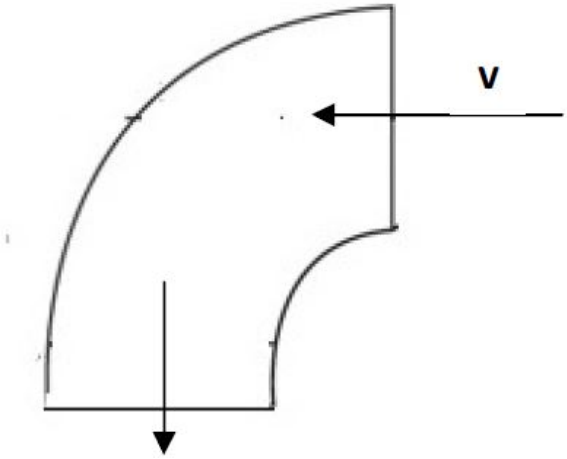

Figure 11.2: Smooth Bend[3]

CFD result and compare it with the experimental or analytical results. The dimensions of the pipe fittings are considered from the lab manual[3]. The simulations were conducted for 17 different cases. To study this turbulent flow, simpleFoam solver is used.

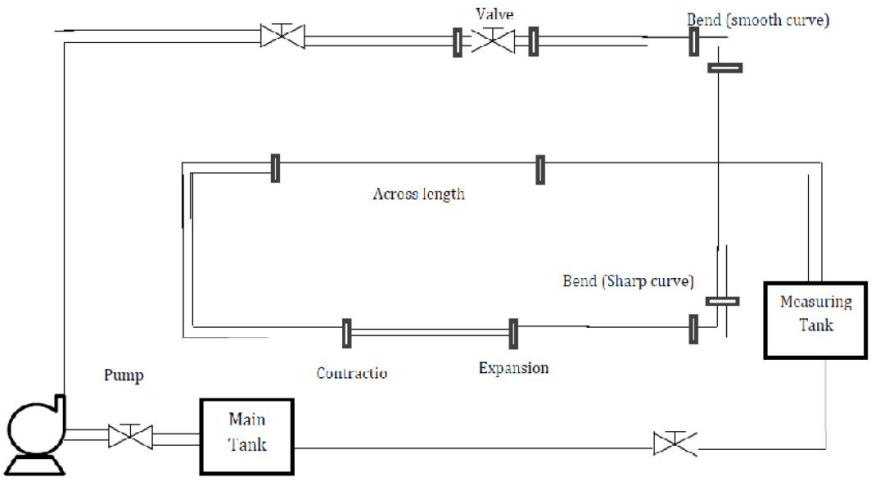

Figure 11.3: Schematic layout of pipe network with fittings[3]

11.4 Schematic Diagram

The dimensions of the geometry is given below
Diameter of the collecting tank, D_c = 0.28 m
Diameter of the larger cross-section pipe, D_1 = 14.3 mm
The geometry of smooth and sharp bend case is shown in the Figure 11.4.

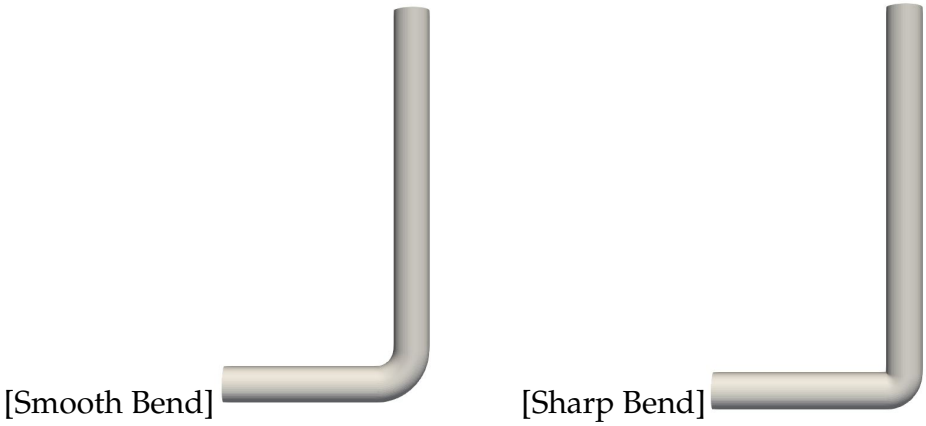

Figure 11.4: Pipe Bend

Chapter 12

OpenFOAM base case

12.1 pitzDaily

The base case considered for the simulation of the orifice meter is the pitzDaily case. This case can be found under the incomressible section, simpleFoam subsection. The directory for this is
\OpenFOAM-v1912\tutorials\incompressible\simpleFoam\pitzDaily.
Based on the experimental work of Pitz and Daily (1981). It features a backward facing step. Such a "classic" case is instructive for comparing different turbulence models with respect to the size and shape of the recirculation zone[internet reference]. pitzDaily introduces the dollowing concepts for the first time:

- Mesh creation using blockMesh and also mesh grading capability
- Turbulent steady flow.

12.1.1 Folder Structure

Any case file in OpenFOAM has three folders, called the 0, constant and the system. The constant contains coefficient values that will be used in equations and also things which will remain constant like the mesh, material properties, environmental constants which the solver uses, the 0 folder contains the initial and boundary conditions, and the system folder contains the configuration files for the mesh and also how the solver will be executed, schemes and methods to use and controls for the simulation.

Table 12.1: Folder contents

Directories	Constant	0	System
Sub-directories	transportProperties turbulenceProperties polyMesh	U p nut omega k	blockMeshDict fvSchemes fvSolution

12.2 Solver

OpenFOAM or Open-source Field Operation And Manipulation is an open-source C++ tool used for solving continuum mechanics problems, with a focus on Finite Volume Method (FVM). The software package includes solver codes for different kinds of transport phenomena, varying from simple laplacian solver called laplacianFoam to complex multiphase flow, compressible flow, heat transfer, incompressible flow, and many more. The flagship solver and most commonly used solver is simpleFoam. simpleFoam is a steady-state solver for incompressible, turbulent flow. It utilizes the SIMPLE (Semi-Implicit Method for Pressure Linked Equations) algorithm. It is an approximation of the velocity field which is obtained by solving the momentum equation. The pressure gradient term is calculated using the pressure distribution from the previous iteration or an initial guess. The pressure equation is formulated and solved to obtain the new pressure distribution. Velocities are corrected and a new set of conservative fluxes is calculated. The solver used for this case study is simpleFoam, it employs SIMPLE algorithm. The case study considered is a steady state, incompressible, three-dimensional flow. The set of Navier Stokes equations governing the flow is given below.
The continuity equation is given as,

$$\nabla.\vec{u} = 0 \tag{12.1}$$

The momentum equation is given as.

$$\frac{\partial \vec{u}}{\partial t} + \nabla.[\vec{u}\vec{u}] = -\frac{1}{\rho}\nabla p + \nu\nabla^2\vec{u} \tag{12.2}$$

Where, $\vec{u}$ is velocity, p-pressure; ν is kinematic viscosity The discretized momentum equation and pressure correction equation are solved implicitly, where the

velocity correction is solved explicitly. This is the reason why it is called "Semi-Implicit Method".

12.2.1 Turbulence Model

The turbulence model considered for the simulation is κ-ω SST RANS model. κ-ω SST model solves two additional equations, for turbulent kinematic energy κ and specific turbulent dissipation rate ω. The equations for the κ-ω SST RANS model is given below,

$$\frac{\partial(p\kappa)}{\partial t} + \frac{\partial(p\kappa u_i)}{\partial x_i} = P - \beta^* \rho\omega\kappa + \frac{\partial}{\partial x_i}[(\mu + \sigma_\omega \mu_t)\frac{\partial\omega}{\partial x_i}] \tag{12.3}$$

$$\frac{\partial(p\omega)}{\partial t} + \frac{\partial(p\omega u_i)}{\partial x_i} = \frac{\gamma}{\nu_t} - \beta\rho\omega^2 + \frac{\partial}{\partial x_i}[(\mu + \sigma_\omega \mu_t)\frac{\partial\omega}{\partial x_i}] + 2(1 - F_1)\frac{\rho\sigma_{\omega 2}}{\omega}\frac{\partial\kappa}{\partial x_i}\frac{\partial\omega}{\partial x_i} \tag{12.4}$$

where u_i represents velocity component in corresponding direction, μ_t represents eddy viscosity. The default value of model coefficients [11] have been used.

Chapter 13

OpenFOAM Case Modifications

Using the pitzDaily case, modifications were made with the geometry, the mesh used, boundary conditions applied to it, and the control parameters which are going to be explained further in the below sections.

13.1 Pre-processing

The models for both the case was created using the dimensions from the manual provided [3]. As the geometry was complicated to be created using blockMesh utility, the geometry and the mesh was created using ANSYS Design Modeller and the mesh using the in-built software. As the geometry has 3-D mesh cells, the upstream length was reduced and a parabolic velocity inlet boundary condition was provided to reduce the computational costs. The downstream length was about 10D.

13.2 Boundary conditions

The initial and boundary conditions are included in the 0 folder as k, omega, nut,p, and U. The boundary conditions are summarised in the Table 13.1 for both the cases. The value for κ and ω were determined using the below equations

$$\kappa = \frac{3}{2}(uI)^2 \tag{13.1}$$

$$\omega = \frac{C_{\mu}^{-0.25}\kappa^{0.5}}{0.07l} \tag{13.2}$$

Table 13.1: Boundary conditions

	inlet	outlet	wall
omega	fixedValue	zeroGradient	omegaWallFunction
k	fixedValue	zeroGradient	kqRWallFunction
nut	calculated	calculated	nutkWallFunction
p	zeroGradient	fixedValue	zeroGradient
U	codedFixedValue	zeroGradient	noSlip

where u is the free stream velocity, I is the turbulence intensity, C_μ is the model coefficient, l is the characteristic length. The inlet velocity was provided through the codedFixedVelocity, parabolic velocity was provided through this function as the upstream length was reduced.

13.3 Physical properties

The working fluid for both the simulation was water. The density considered was 1000 kg/ m^3, with a kinematic viscosity of 1×10^{-06} $m^2/\ s$. The value in the transportProperties file was changed to 1×10^{-06} from 1×10^{-05} and the transportModel remained as it is to Newtonian.

13.4 fvSchemes & fvSolution

fvSchems and fvSolutions are found under the constant folder. fvSolution directory contains equation solvers, algorithms and tolerances. No changes were done to this file, the tolerances for the residuals were pre-set to a value of 1e-05 and it was not changed. The numerical schemes for the simulation are entered in the fvSchemes dictionary. No changes were made in this file directory.

13.5 Control parameters

The OpenFOAM solvers begin all runs by setting up a database. The database controls I/O and, since output of data is usually requested at intervals of time during the run, time is an inextricable part of the database. The controlDict dictionary

sets input parameters essential for the creation of the database. Here the endTime was changed to 4000, i.e., maximum iterations were 4000. startTime was 0 and writeInterval was set to every 100 iterations with 1 as deltaT as it was a steady state analysis.

13.6 Post-processing

After the simulation has been completed, the results were viewed in ParaView. To do this, first the results obtained were converted into viewable file using the command *touch suitable_file_name.foam*. A file with .foam extension was created. In this file, the results was viewed, the various contours of the solution was visualised, streamlines were plotted and the data were analysed with the in-built plotting options available.

Chapter 14

Results

Steady state simulations were performed using SIMPLE algorithm for κ-ω SST RANS model. The obtained CFD results have been compared with the experimental results for the coefficient of discharge. Post-processing was done using paraview.

14.1 Numerical Results

The post-processing of the simulation was done in ParaView for both the cases each having 17 simulations, the Reynolds number varied from 5000 to 26000. The numerical results are further discussed below.

14.1.1 Smooth Bend

The velocity and pressure contours obtained by the simulations are shown in Figure 14.1. Also, the pressure and velocity contours for higher and lower Reynolds number are also plotted in Figure 14.2 and Figure 14.3. From the contours it is seen that at the bend, there is a change in the direction of the velocity, which leads to boundary layer separation. Due to the effect of centrifugal force, the boundary layer at the inner wall is getting thicker and the boundary layer at the outer wall is getting thinner. When the centrifugal force continues to increase, the boundary layer will separate from the inner wall[12]. Due to this separation, there is a loss in head, which accounts for the minor loss.

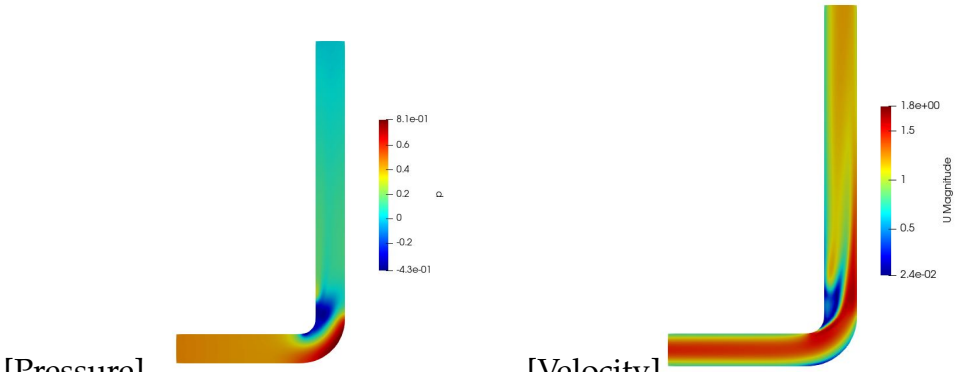

[Pressure] [Velocity]

Figure 14.1: Contours

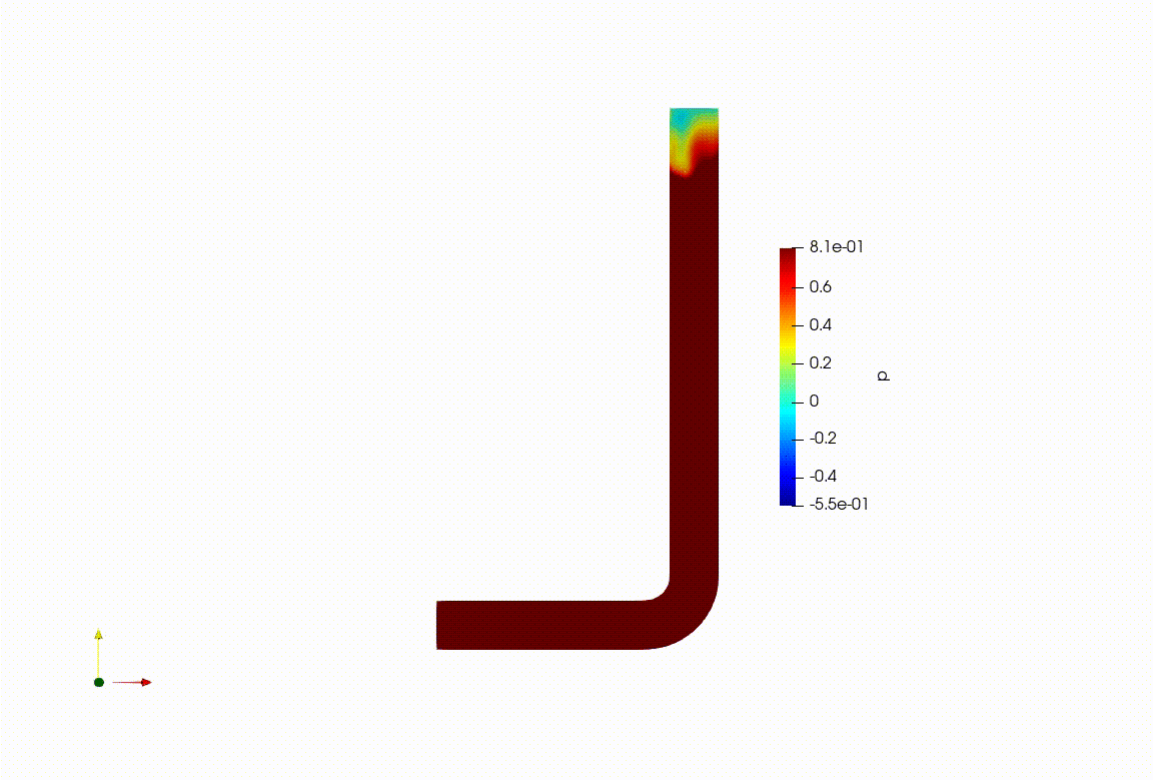

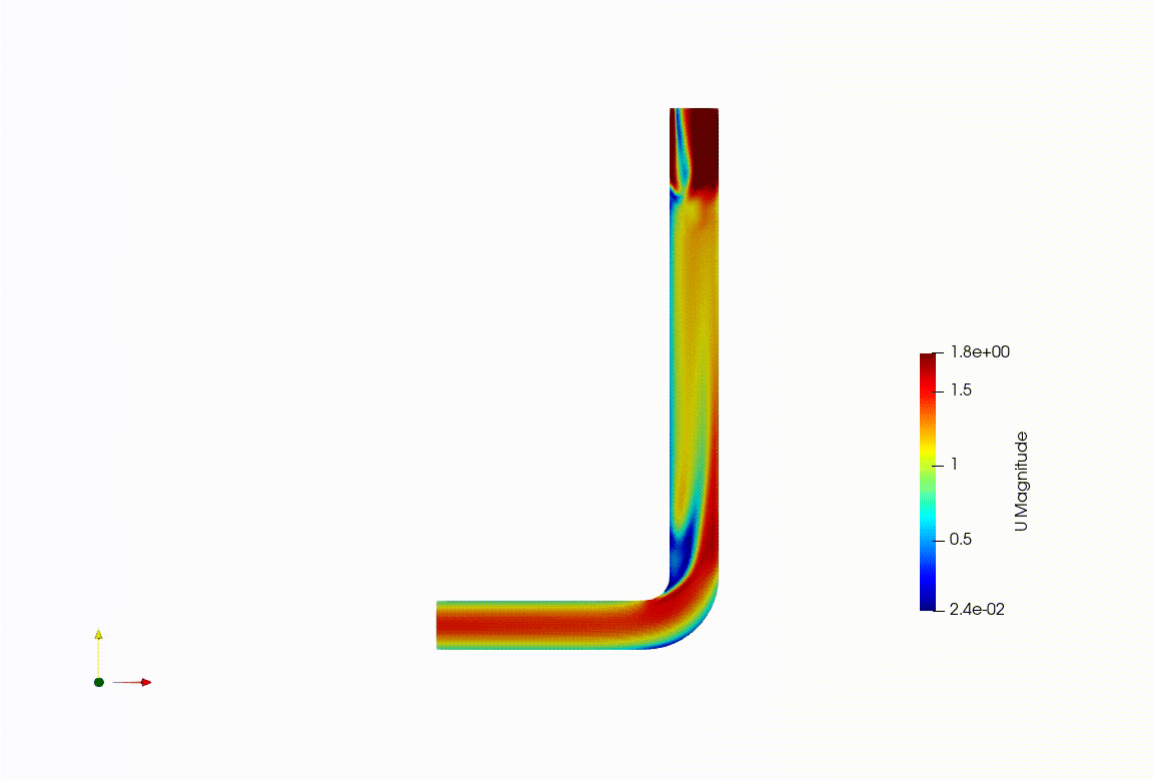

[High Reynolds] [Low Reynolds]

Figure 14.2: Pressure Contour

Due to the flow separation and centrifugal forces, there is a secondary flow pattern occurring at the exit of the bend. The secondary flow features include pair of counter-rotating stream-wise vortices called Dean vortices. These flow structure are further shown in the Figure 14.4. The stream-wise vortices formed are circled in red colour. Dean vortices are also plotted for higher and lower Reynolds number and are shown in Figure 14.5 and Figure 14.6 respectively. It is seen that the Dean

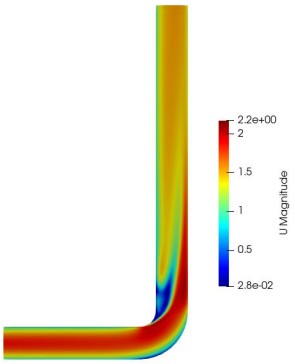

[High Reynolds]

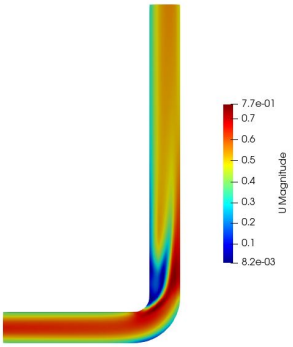

[Low Reynolds]

Figure 14.3: Velocity Contour

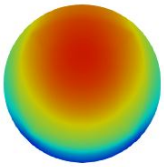

[Entrance]

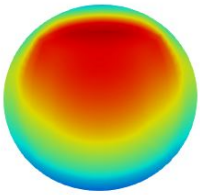

[45^o]

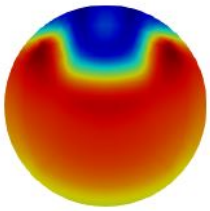

[Exit]

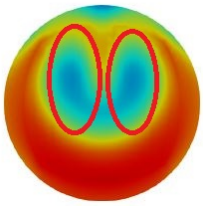

[6D]

Figure 14.4: Dean vortices

vortices formed for higher Reynolds number is unsymmetrical compared to the lower Reynolds number case.

14.1.2 Sharp Bend

The velocity and pressure contours obtained by the simulations are shown in Figure 14.7. Also, the pressure and velocity contours for higher and lower Reynolds number are also plotted from Figure 14.8 and Figure 14.9. From the contours it is seen that for sharp bend, the change in the direction of the velocity is greater compared to smooth bend, which leads to larger boundary layer separation compared to smooth bend. As the separation is greater, it leads greater loss in pressure head and in turn greater minor loss compared to smooth bend.

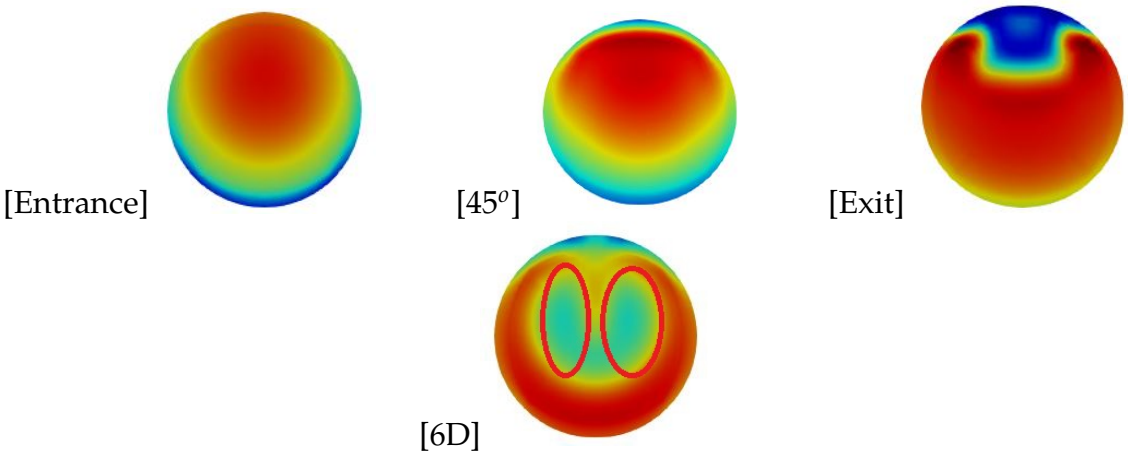

Figure 14.5: Dean vortices for Higher Reynolds number

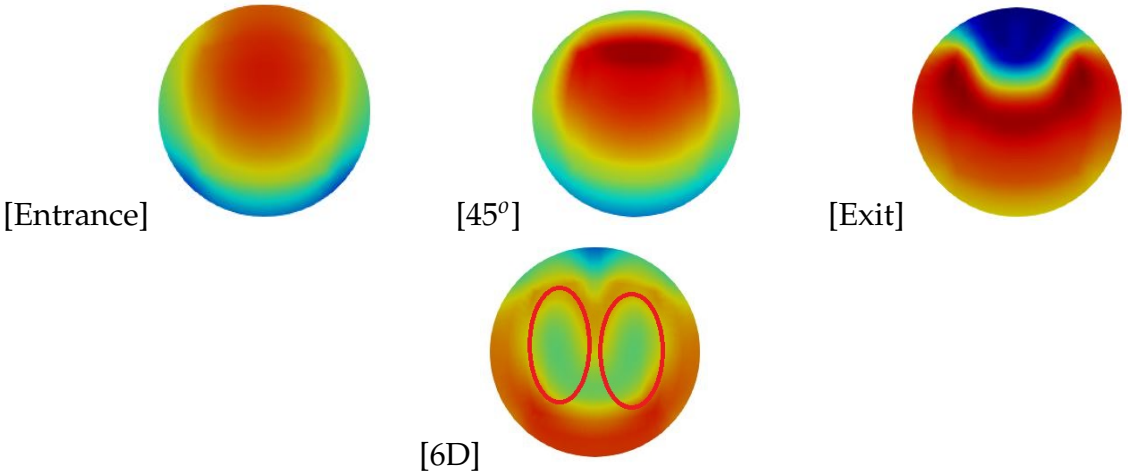

Figure 14.6: Dean vortices for Lower Reynolds number

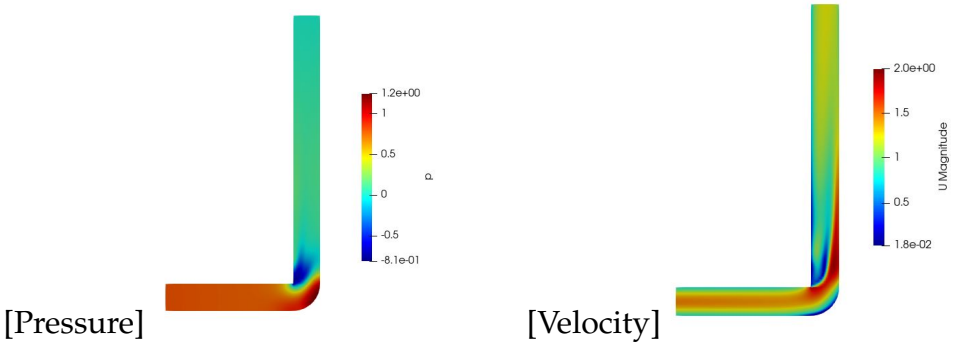

Figure 14.7: Contours

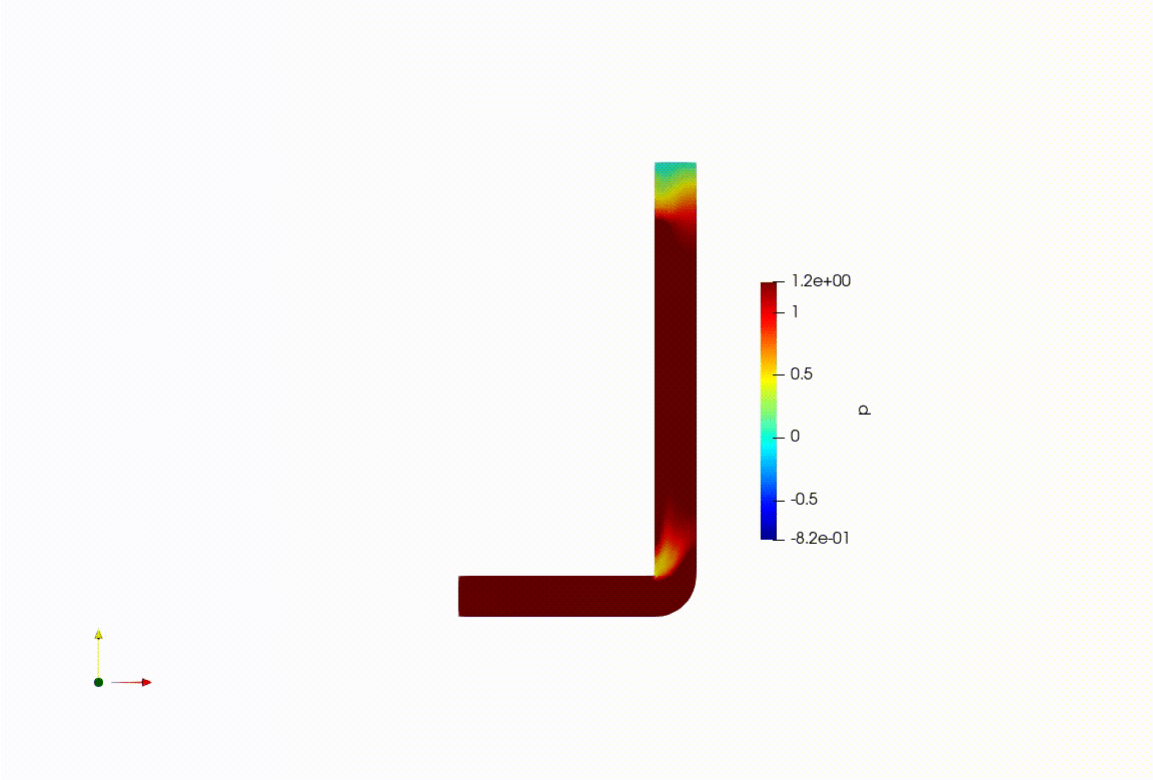

[High Reynolds]

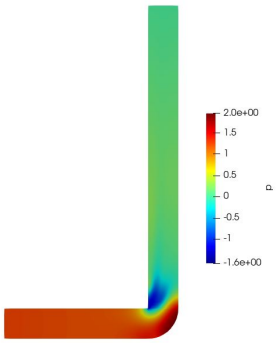

[Low Reynolds]

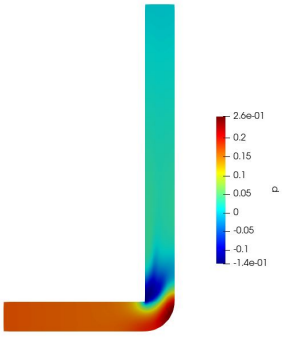

Figure 14.8: Pressure Contour

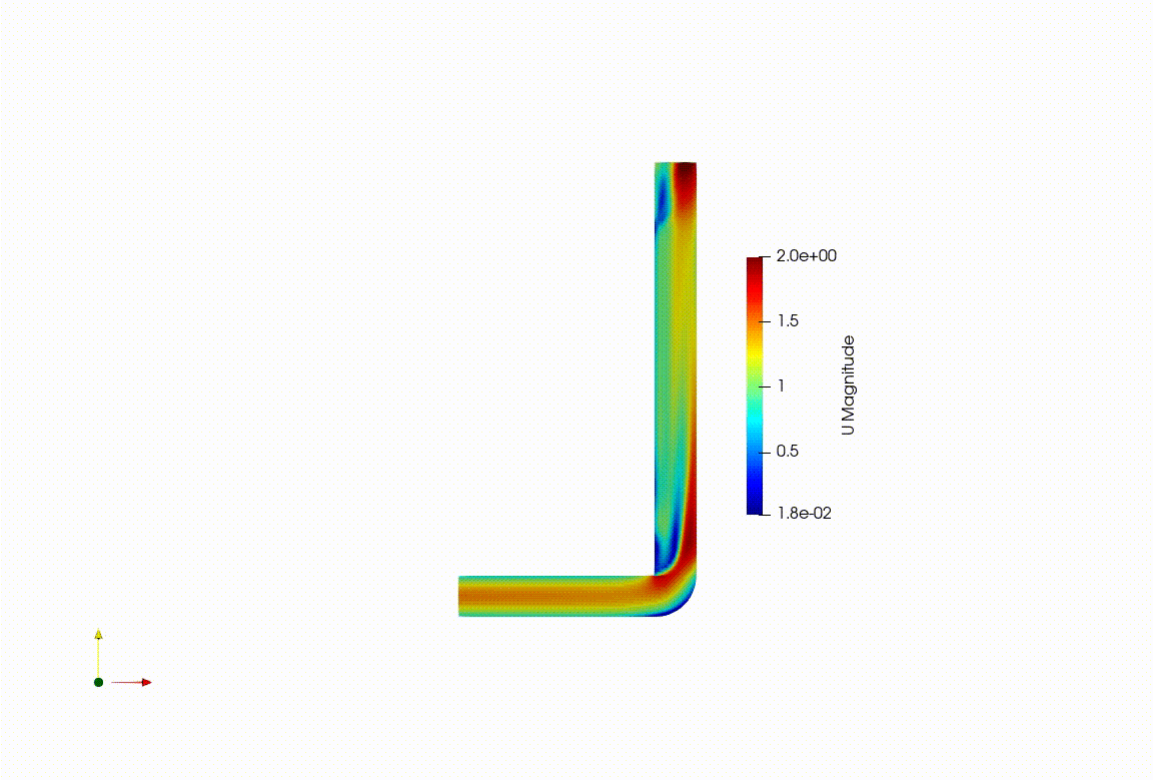

[High Reynolds]

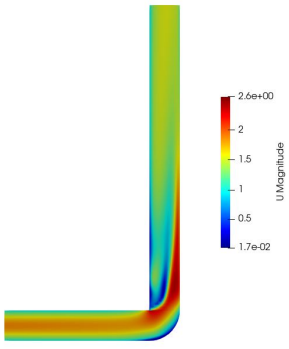

[Low Reynolds]

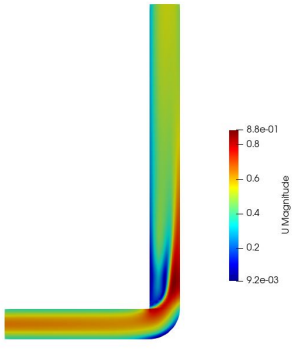

Figure 14.9: Velocity Contour

Due to the flow separation and centrifugal forces, there is a secondary flow pattern occurring at the exit of the bend. The secondary flow features include pair of counter-rotating stream-wise vortices called Dean vortices. These flow structure are further shown in the Figure 14.10. The stream-wise vortices formed here are similar to the ones that were formed in the smooth bend. These are also plotted for higher and lower Reynolds number and are shown in Figure 14.11 and Figure 14.12

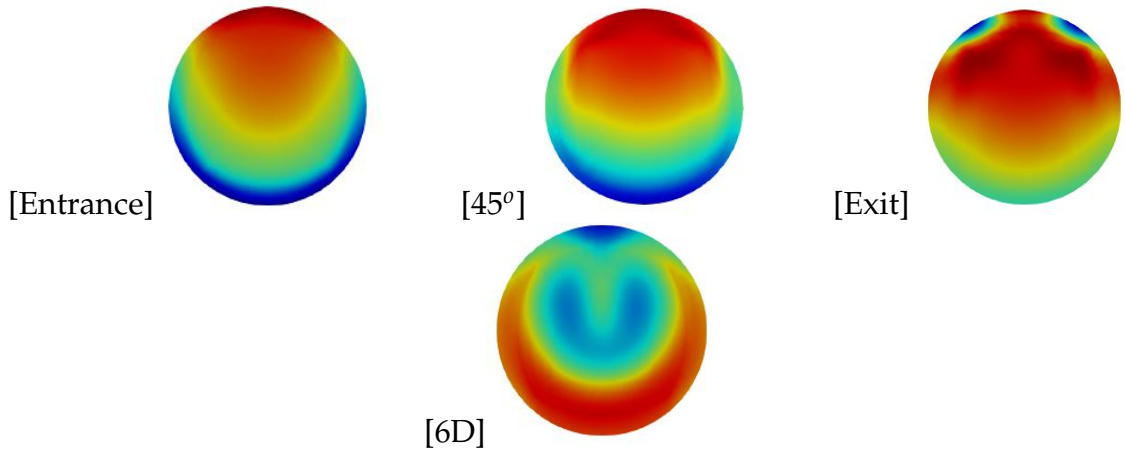

Figure 14.10: Dean vortices

respectively. Again, it is seen that the Dean vortices formed for higher Reynolds number is unsymmetrical compared to the lower Reynolds number case.

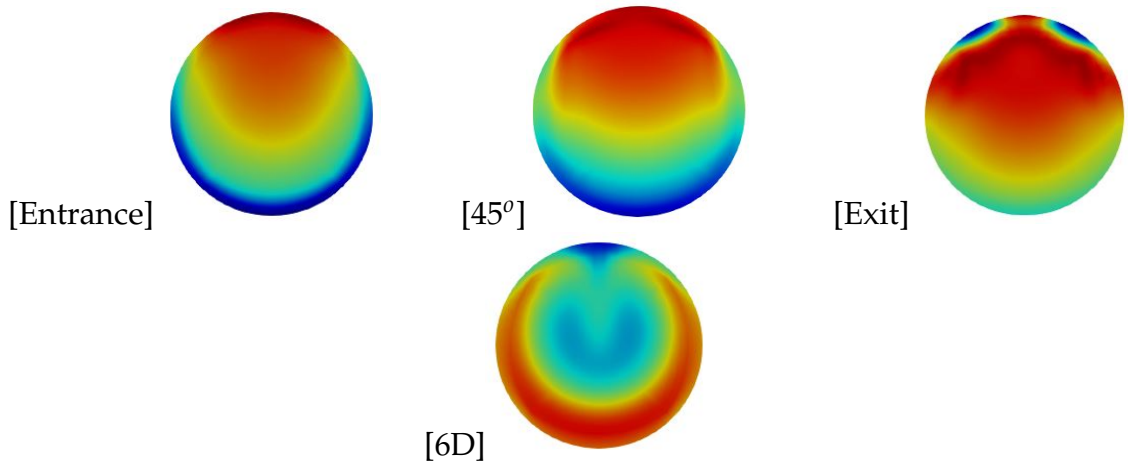

Figure 14.11: Dean vortices for Higher Reynolds number

14.1.3 Minor Loss Factors

The minor loss factors are determined for both the cases using the Equation 11.4 for both the cases. The pressure difference for the equation, was determined between the entrance of the bend and at a distance of 9D from the exit of the end as suggested in the paper[13]. To ensure the method was right, the minor pressure difference available in the literature was reproduced through CFD simulations and were

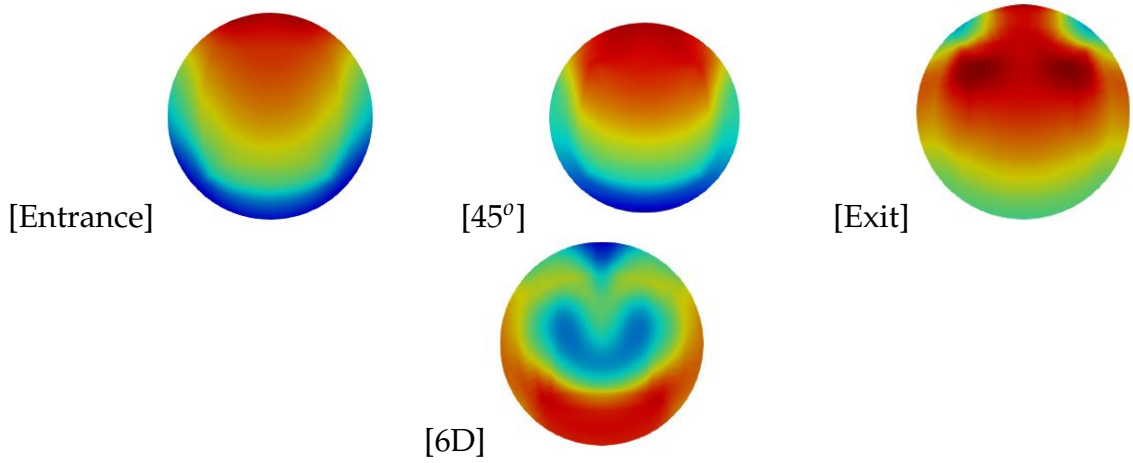

Figure 14.12: Dean vortices for Lower Reynolds number

compared. The obtained values are summarised in Table 14.1. From Table 14.1 it is

Table 14.1: Literature Values v/s CFD values

Velocity	Reynolds Number	k (CFD)	k (Exp)	Error
1	40000	0.224	0.26	13.84
2	80000	0.185	0.163	13.49
3	120000	0.1705	0.1429	19.31
5	200000	0.1552	0.1396	11.17

seen that the error between CFD and published value is less which assures the procedure through which the pressure difference obtained is right. With this, minor losses for both smooth and sharp bend is determined and is summarised in Table 14.2 and Table 14.3 respectively.

Table 14.2: CFD results for smooth bend

Sl No.	Flow rate(m^3/s)	Velocity (m/s)	Reynolds number	Turbulent kinetic energy (m^2/s^2)	Specific dissipation rate (s^{-1})	Pressure difference	K
1	0.000237	1.478038	21021	0.006858	151.0441	0.3705	0.343
2	0.000236	1.469798	20878	0.0068	150.4041	0.3625	0.3401
3	0.000202	1.25876	17875	0.00518	131.2714	0.2733	0.349
4	0.00021	1.307589	18590	0.00555	135.8788	0.29543	0.3496
5	0.000194	1.210081	17303	4.901e-3	127.6872	0.2552	0.3489
6	0.000182	1.132066	16159	4.348e-3	120.2679	0.2249	0.3524
7	0.000301	1.872526	26741	0.0105	186.8959	0.5445	0.3114
8	0.000294	1.831351	26169	0.0101	183.3014	0.5257	0.3139
9	0.000283	1.760117	25168	9.4437e-3	177.2459	0.4903	0.3165
10	0.000277	1.727316	24596	9.071e-3	173.7132	0.4693	0.3173
11	0.000288	1.792788	25597	9.727e-3	179.8849	0.5063	0.316
12	0.000291	1.812293	25883	9.918e-3	181.6424	0.5122	0.3127
13	0.000105	0.653563	9345.05	1.65e-3	74.0878	0.0849	0.402
14	0.000147	0.915238	13013	2.9772e-3	99.5197	0.1609	0.3887
15	9.88E-05	0.615353	8723	1.4785e-3	70.1319	0.085	0.4573
16	0.000106	0.659413	9295	1.6523e-3	74.1395	0.085	0.4028
17	6.29E-05	0.391737	5577	6.7586e-4	47.4169	0.03507	0.4611

Table 14.3: CFD results for sharp bend

Sl No.	Flow rate(m^3/s)	Velocity (m/s)	Reynolds number	Turbulent kinetic energy (m^2/s^2)	Specific dissipation rate (s^{-1})	Pressure difference	K
1	0.000237	1.478038	21021	0.006858	151.0441	0.607	0.5618
2	0.000236	1.469798	20878	0.0068	150.4041	0.607	0.5695
3	0.000202	1.25876	17875	0.00518	131.2714	0.4430	0.5671
4	0.00021	1.307589	18590	0.00555	135.8788	0.4783	0.566
5	0.000194	1.210081	17303	4.901e-3	127.6872	0.4158	0.5681
6	0.000182	1.132066	16159	4.348e-3	120.2679	0.364	0.5701
7	0.000301	1.872526	26741	0.0105	186.8959	0.9043	0.5172
8	0.000294	1.831351	26169	0.0101	183.3014	0.8671	0.5178
9	0.000283	1.760117	25168	9.4437e-3	177.2459	0.8031	0.5185
10	0.000277	1.727316	24596	9.071e-3	173.7132	0.7677	0.5190
11	0.000288	1.792788	25597	9.727e-3	179.8849	0.8298	0.5179
12	0.000291	1.812293	25883	9.918e-3	181.6424	0.8487	0.5181
13	0.000105	0.653563	9345.05	1.65e-3	74.0878	0.1328	0.6289
14	0.000147	0.915238	13013	2.9772e-3	99.5197	0.2545	0.6146
15	9.88E-05	0.615353	8723	1.4785e-3	70.1319	0.1176	0.6323
16	0.000106	0.659413	9295	1.6523e-3	74.1395	0.1327	0.6285
17	6.29E-05	0.391737	5577	6.7586e-4	47.4169	0.0512	0.674

Chapter 15

Conclusion

In this case study, simulation of turbulent flow through smooth and sharp bend was done using κ-ω SST RANS turbulence model.The minor loss factor was determined for both the cases in Reynolds number range of 5000-26000. Velocity, pressure contours and secondary flow features were visualised through which various distinctive flow behaviours were studied.

Bibliography

[1] Serajuddin Ansari, M Siva, and Sayedahammad. What is an orifice meter ? - instrumentationtools, Jul 2019.

[2] *Flow Measurement by Venturimeter and orifice meter, Thermofluids Lab Manual, Department of Energy Science and Engineering, IIT Bombay.*

[3] *Losses due to Pipe Fittings, Thermofluids Lab Manual, Department of Energy Science and Engineering, IIT Bombay.*

[4] Warren Lee McCabe, Julian Cleveland Smith, and Peter Harriott. *Unit operations of chemical engineering*, volume 5. McGraw-hill New York, 1993.

[5] Frank M White and Isla Corfield. *Viscous fluid flow*, volume 3. McGraw-Hill New York, 2006.

[6] DR Laurence, JC Uribe, and SV Utyuzhnikov. A robust formulation of the v2-f model. *Flow, Turbulence and Combustion*, 73(3):169–185, 2005.

[7] MM Tukiman, MNM Ghazali, A Sadikin, NF Nasir, N Nordin, A Sapit, and MA Razali. Cfd simulation of flow through an orifice plate. In *IOP Conference Series: Materials Science and Engineering*, volume 243, page 012036. IOP Publishing, 2017.

[8] Manish S Shah, Jyeshtharaj B Joshi, Avtar S Kalsi, CSR Prasad, and Daya S Shukla. Analysis of flow through an orifice meter: Cfd simulation. *Chemical engineering science*, 71:300–309, 2012.

[9] Baoyu Guo, Tim AG Langrish, and David F Fletcher. Cfd simulation of precession in sudden pipe expansion flows with low inlet swirl. *Applied Mathematical Modelling*, 26(1):1–15, 2002.

[10] Manmatha K Roul and Sukanta K Dash. Two-phase pressure drop caused by sudden flow area contraction/expansion in small circular pipes. *International journal for numerical methods in fluids*, 66(11):1420–1446, 2011.

[11] Florian R Menter. Two-equation eddy-viscosity turbulence models for engineering applications. *AIAA journal*, 32(8):1598–1605, 1994.

[12] Yan Wang, Quanlin Dong, and Pengfei Wang. Numerical investigation on fluid flow in a 90-degree curved pipe with large curvature ratio. *Mathematical Problems in Engineering*, 2015, 2015.

[13] Máté Bíbok, Péter Csizmadia, and Sára Till. Experimental and numerical investigation of the loss coefficient of a 90 pipe bend for power-law fluid. *PERIODICA POLYTECHNICA-CHEMICAL ENGINEERING*, 64(4):469–478, 2020.